

1 Reconciling the Cretaceous breakup and demise of the Phoenix 2 Plate with East Gondwana orogenesis in New Zealand

3

4 Suzanna H.A. van de Lagemaat^{1,*}, Peter J.J. Kamp², Lydian M. Boschman¹, Douwe J.J. van
5 Hinsbergen¹

6

7 ¹ Department of Earth Sciences, Utrecht University, Utrecht, the Netherlands

8 ² School of Science, University of Waikato, Hamilton, New Zealand

9

10 * Corresponding author: Suzanna van de Lagemaat (s.h.a.vandelagemaat@uu.nl)

11

12 **Highlights**

- 13 - GPlates reconstruction of the South Pacific realm back to 150 Ma
- 14 - Pacific Plate-Zealandia convergence continued until 90-85 Ma
- 15 - Subduction along the Zealandia margin may have continued until 79 Ma accommodated
16 by Osbourn Trough spreading
- 17 - Reconstruction reveals ridge subduction rather than subduction termination as possible
18 cause of a 105-100 Ma change in magmatic arc signature in Zealandia

19

20 **Keywords:** East Gondwana subduction zone, plate tectonics, GPlates, kinematic plate
21 reconstruction, New Zealand, New Caledonia, Zealandia

22

23 **This paper is a non-peer reviewed manuscript submitted to EarthArXiv. The manuscript**
24 **has been submitted for peer review to *Earth-Science Reviews***

25 **Abstract**

26 Following hundreds of millions of years of subduction in all circum-Pacific margins, the Pacific
27 Plate started to share a mid-ocean ridge connection with continental Antarctica during a Late
28 Cretaceous south Pacific plate reorganization. This reorganization was associated with the
29 cessation of subduction of the remnants of the Phoenix Plate along the Zealandia margin of East
30 Gondwana, but estimates for the age of this cessation from global plate reconstructions (~86
31 Ma) are significantly younger than those based on overriding plate geological records (105-100
32 Ma). To find where this discrepancy comes from, we first evaluate whether incorporating the
33 latest available marine magnetic anomaly interpretations change the plate kinematic estimate
34 for the end of convergence. We then identify ways to reconcile the outcome of the
35 reconstruction with geological records of subduction along the Gondwana margin of New
36 Zealand and New Caledonia. We focus on the plate kinematic evolution of the Phoenix Plate
37 from 150 Ma onward, from its original spreading relative to the Pacific Plate, through its break-
38 up during emplacement of the Ontong Java Nui Large Igneous Province into four plates
39 (Manihiki, Hikurangi, Chasca, and Aluk), through to the end of their subduction below East
40 Gondwana, to today. Our updated reconstruction is in line with previous compilations in
41 demonstrating that as much as 800-1100 km of convergence occurred between the Pacific Plate
42 and Zealandia after 100 Ma, which was accommodated until 90-85 Ma. Even more convergence
43 occurred at the New Zealand sector owing to spreading of the Hikurangi Plate relative to the
44 Pacific Plate at the Osbourn Trough, with the most recent age constraints suggesting that
45 spreading may have continued until 79 Ma. The end of subduction below most of East
46 Gondwana coincides with a change in relative plate motion between the Pacific Plate and East
47 Gondwana from westerly to northerly, of which the cause remains unknown. In addition, the
48 arrival of the Hikurangi Plateau in the subduction zone occurred independent from, and did not
49 likely cause, the change in Pacific Plate motion. Finally, our plate reconstruction suggests that
50 the previously identified geochemical change in the New Zealand arc around 105-100 Ma that
51 was considered evidence of subduction cessation, may have been caused by Aluk-Hikurangi
52 ridge subduction instead. The final stages of convergence before subduction cessation must
53 have been accommodated by subduction without or with less accretion. This is common in
54 oceanic subduction zones but makes dating the cessation of subduction from geological records
55 alone challenging.

56 **1. Introduction**

57 During the Late Cretaceous, an important tectonic change occurred in the southern
58 Pacific realm. For hundreds of millions of years, including most of the Mesozoic, the Panthalassa
59 (or Paleo-Pacific) Ocean was surrounded by subduction zones that consumed oceanic
60 lithosphere of the Farallon (NE), Izanagi (NW), and Phoenix (S) plates (e.g., Engebretson et al.
61 1985; Seton et al., 2012; Wright et al., 2016; Müller et al., 2019; Torsvik et al., 2019; Boschman
62 et al., 2021a). During the Cretaceous, however, subduction ended along the Zealandia sector of
63 the East Gondwana continental margin (e.g., Bradshaw, 1989; Luyendyk, 1995; Davy et al.,
64 2008; Matthews et al., 2012). Sections of the suture of the Mesozoic subduction zone are located
65 along the northern margin of the Chatham Rise and along the Thurston Island sector of
66 Antarctica, which are presently separated from each other by the Pacific-Antarctic Ridge (Fig.
67 1). This implies that when Pacific-Antarctic spreading started, the ridge did not simply replace
68 the former East Gondwana subduction zone. Instead, it cut through the subduction zone suture
69 and formed partly intra-oceanic and partly intra-continental within East Gondwana lithosphere
70 (Larter et al., 2002; Wobbe et al., 2012). Around the time of subduction cessation, several
71 oceanic plates that formed after breakup of the Phoenix Plate, as well as part of Zealandia,
72 merged with the Pacific Plate. Since then, the Pacific Plate has been diverging from West
73 Antarctica, accommodated by oceanic spreading at the Pacific-Antarctic Ridge (Fig. 1B). But
74 despite its importance in the plate tectonic history of the Panthalassa/Pacific domain, the
75 southwest Pacific-East Gondwana plate reorganization is surrounded with uncertainty.

76 The uncertainty surrounding the southwest Pacific-East Gondwana plate reorganization
77 results from a discrepancy in the age of subduction cessation between different studies. On the
78 one hand, geologists studying the magmatism and deformation in the orogen located at the
79 overriding plate margin of New Zealand have found no conclusive evidence that shows that
80 subduction must have continued beyond 105-100 Ma (e.g., Bradshaw, 1989; Luyendyk, 1995;
81 Mortimer et al., 2019; Crampton et al., 2019). A 105-100 Ma age estimate for subduction
82 cessation is commonly inferred from a change in deformation within New Zealand from largely
83 compression to a regime dominated by extension (e.g., Bradshaw, 1989; Luyendyk, 1995;
84 Crampton et al., 2019), coeval changes in the geochemical signature of magmatism (Muir et al.,
85 1997; Waight et al., 1998; Tulloch and Kimbrough, 2003; Tulloch et al., 2009; Van der Meer et
86 al., 2016; 2017; 2018), and angular unconformities in the New Zealand forearc (Laird and
87 Bradshaw, 2004; Crampton et al., 2019; Gardiner et al., 2021; 2022). On the other hand, global
88 plate reconstructions suggest that convergence across the Zealandia margin of New Zealand
89 continued until at least the end of spreading in the Osborn Trough, of which estimates vary
90 from ~101 Ma to 79 Ma, based on dredge samples and tentative marine magnetic anomaly
91 identification (Billen and Stock, 2000; Worthington et al., 2006; Seton et al., 2012; Zhang and Li,

92 2016; Mortimer et al., 2019), with widely-used global plate reconstructions (Seton et al., 2012;
93 Matthews et al., 2016; Müller et al., 2019) inferring an 86 Ma age that follows Worthington et al.
94 (2006). This age, however, is based on interpretations of the New Zealand geological record that
95 is disputed by many geologists that study New Zealand (e.g., Crampton et al., 2019; Mortimer et
96 al., 2019). Reconciling the geological and plate kinematic estimates of the age of subduction
97 cessation therefore requires using kinematic data from the oceanic and continental domain that
98 are independent from interpreted ages of subduction cessation to avoid circular reasoning in
99 making reconstruction choices.

100 To do so, we analyse the end of East Gondwana subduction along the Zealandia margin
101 by reassessing both the plate kinematic and orogenic perspectives. First, we evaluate whether
102 the age for the end of convergence suggested by global plate models changes by using the latest,
103 and most detailed published marine magnetic anomaly-based isochrons, and by using the range
104 of estimates for the arrest of Osbourn Trough spreading based on magnetic anomalies or dredge
105 samples. Our reconstruction includes the evolution and fragmentation of the Phoenix Plate into
106 its several daughter plates. We use the recent study of Torsvik et al. (2019) who revisited and
107 modified absolute Pacific Plate models and updated earlier global plate reconstructions. We
108 consider relative motions across the East Gondwana continental margin as a function of
109 absolute plate motion models to evaluate when convergence may have ended, and which
110 process may have been responsible for this cessation. Furthermore, we review aspects of the
111 architecture and evolution of the Cretaceous New Zealand orogen, and attempt to reconcile the
112 timing of the end of subduction with the available geological evidence. We will use our results as
113 a basis for the reconstruction of the demise of the Phoenix Plate's daughters, which resulted
114 from their capture by the Pacific Plate after cessation of subduction along the Gondwana margin
115 and the enigmatic transition to the Pacific-Antarctic spreading ridge.

116

117 **2. Plate tectonic setting**

118 The south Pacific Ocean today is underlain by the Pacific, Antarctic, and Nazca plates,
119 separated by trenches from the South American, Antarctic, and Australian plates (Fig. 1). The
120 oceanic plates of the Pacific Ocean are separated from each other by mid-ocean ridges: the
121 Pacific-Antarctic Ridge, the East Pacific Rise between the Pacific and Nazca plates, and the Chile
122 Ridge between the Antarctic and Nazca plates (Fig. 1). Three microplates are present along the
123 East Pacific Rise: The Juan Fernandez, Easter, and Galapagos microplates.

124 In the west, the Pacific Plate is currently subducting below the Australian Plate at the
125 Tonga-Kermadec-Hikurangi subduction zone. To the west of this subduction zone is a series of
126 Cenozoic back-arc basins (e.g., Lau Basin, South Fiji Basin, Norfolk Basin; e.g., Yan and Kroenke,
127 1993; Sdrolias et al., 2003; Herzer et al., 2011), bounded in the west by the extended continental

128 crust of Zealandia that underlies the Lord Howe Rise and Norfolk Ridge (e.g., Mortimer et al.,
129 2017). Zealandia is separated from the Australian continent by the Upper Cretaceous-Paleogene
130 Tasman Sea and New Caledonia basins (e.g., Gaina et al., 1998; Grobys et al., 2008). The Norfolk
131 Ridge was overthrust from the east during the Oligocene (c. 30 Ma) by the Paleocene New
132 Caledonia ophiolite (Cluzel and Meffre, 2002; Cluzel et al., 2012). Ophiolite obduction occurred
133 during cessation of a northeast-dipping intra-oceanic subduction zone that formed around 60
134 Ma. At this time other ophiolites also formed that were emplaced during the Late Oligocene onto
135 Northland, New Zealand, and northward towards the Louisiade Plateau and the eastern Papuan
136 Peninsula (Fig. 1) (Whattam et al., 2006; Cluzel et al., 2012; Van de Lagemaat et al., 2018a;
137 Maurizot et al., 2020a; McCarthy et al., 2022).

138 At its northern end, southwest of Samoa, the Tonga-Kermadec-Hikurangi subduction
139 turns sharply to the west (Fig. 1). Here the plate boundary changes to a SW-trending, diffuse
140 transform system around the Fiji Islands, southwest of which it continues as the Hunter fracture
141 zone that connects to the New Hebrides Trench. At this trench the Australian Plate is subducting
142 below the North Fiji back-arc basin that hosts spreading ridges with the Pacific Plate. The
143 southern end of the Tonga-Kermadec-Hikurangi subduction zone connects via the right-lateral
144 Alpine Fault to the Puysegur Trench where subduction of the Australian Plate below the Pacific
145 Plate is occurring (e.g., Collot et al., 1995; House et al., 2002; Gurnis et al., 2019). The plate
146 boundary ends at the Macquarie Triple Junction, where the Australian, Pacific, and Antarctic
147 plates meet, and where the Macquarie microplate formed c. 7 Ma (Cande and Stock, 2004a; Choi
148 et al., 2017). Kinematic reconstructions of Cenozoic tectonic history of the SW Pacific realm
149 differ in the timing and distribution of convergence over the New Caledonia and Tonga-
150 Kermadec subduction zones (Hall, 2002; Schellart et al., 2006; Whattam et al., 2008; Van de
151 Lagemaat et al., 2018a), but mostly agree on the pre-late Cretaceous position of Zealandia
152 against the Australian continent, and on the location of the subduction zone along the eastern
153 Zealandia margin that consumed the Phoenix Plate and its daughters (Fig. 2).

154 The southern boundary of the Pacific Plate is the Pacific-Antarctic Ridge (Fig. 1B). This
155 plate boundary formed c. 89 Ma, based on the extrapolation of spreading rates from the oldest
156 identified marine magnetic anomaly (C34y; 83.7 Ma) towards the continental margin (Wobbe et
157 al., 2012). This age is in correspondence with the 83.9 ± 0.1 Ma age of the Erik seamount,
158 obtained from Ar/Ar dating of K-feldspar of a trachyte sample, which provides a minimum age
159 of the oceanic crust (Mortimer et al., 2019). The Pacific-Antarctic Ridge accommodated the
160 divergence of the Campbell Plateau (part of the Zealandia continent, located on the Pacific Plate)
161 from Marie Byrd Land (located on the West Antarctic Plate) (e.g., Wobbe et al., 2012). Before
162 break-up, the Campbell Plateau and West Antarctica formed part of the upper plate adjacent to
163 the Mesozoic active margin of East Gondwana (Fig. 2) (e.g., Larter et al., 2002). This margin was

164 contiguous with the active margins of the Antarctic Peninsula and South America, where
165 subduction remains active today. Presently, subduction of a small remnant of the last of the
166 Phoenix Plate's daughters, the Aluk Plate (Herron and Tucholke, 1976), is ongoing below the
167 northern part of the Antarctic Peninsula (Fig. 1) (e.g. Eagles, 2004). The Aluk Plate is often also
168 referred to as Phoenix Plate, but we prefer the name Aluk Plate to make the distinction with the
169 original parent Phoenix Plate. Subduction below Antarctica progressively ceased with the
170 arrival of different segments of the Aluk-Antarctica Ridge. A small segment of this ridge remains
171 in the Southeast Pacific Ocean, which became extinct c. 3.3 Ma (Eagles, 2004), effectively
172 merging the Aluk Plate with the Antarctic Plate. Subduction below the Antarctic Peninsula is
173 currently accommodated by opening of the Bransfield Basin within the upper Antarctic Plate
174 (Fig. 1; Galindo-Zaldívar et al., 2004). The eastern boundary of the Aluk Plate is the Shackleton
175 Fracture Zone, separating it from the West Scotia Sea. Opening of the Scotia Sea oceanic basins
176 was not related to plate motions of the paleo-Pacific realm (Van de Lagemaat et al., 2021) and
177 the Shackleton Fracture Zone is thus the eastern boundary of our reconstruction. To the north
178 of the Shackleton Fracture Zone, the Antarctic Plate, Chile Ridge, and Nazca Plate are subducting
179 below South America.

180 Mesozoic subduction of Phoenix Plate lithosphere was accommodated along the
181 Antarctica and Zealandia margins of East Gondwana (Fig. 2). Breakup of these continents from
182 each other and from Australia led to oceanic spreading around 84 Ma in both the Tasman Sea
183 and South Pacific Ocean (Gaina et al., 1998; Wobbe et al., 2012; Mortimer et al., 2019), but
184 continental rifting between Zealandia and Antarctica and between Zealandia and Australia has
185 been considered to date back to c. 105-100 Ma (Bradshaw, 1989; Luyendyk, 1995; Laird and
186 Bradshaw, 2004). Earliest extension between Australia and Antarctica started at c. 136 Ma
187 (Whittaker et al., 2013).

188 A prominent record of Mesozoic subduction is present in New Zealand. The Eastern
189 Province consists of Permian intra-oceanic arc sequences and a long-lived Mesozoic
190 accretionary wedge (Fig. 3) (Mortimer, 2004; Mortimer et al., 2014). It is possible that the
191 Eastern Province hosts the records of two subduction systems, one along the Gondwana margin
192 and one intra-oceanic (Adams et al., 2007; Van de Lagemaat et al., 2018b; Campbell et al., 2020),
193 but these have been juxtaposed since at least the latest Jurassic (Tulloch et al., 1999), i.e.,
194 throughout the window of interest of this paper. The western and eastern provinces are
195 separated by the Median Batholith that represents a long-lived Paleozoic to Mesozoic magmatic
196 arc (Fig. 2 and 3) (Mortimer, 2004). The accretionary wedge of the Eastern Province consists of
197 ocean plate stratigraphy (OPS; Isozaki et al., 1990) comprising pillow lavas, oceanic pelagic and
198 hemipelagic sediments, and trench fill clastics (Caples, Waipapa and Torlesse terranes;
199 Mortimer et al., 2014). These OPS sequences accreted to the Gondwana margin from Permian to

200 Early Cretaceous times and were intruded by magmatic arc plutons and overlain by forearc
201 basin clastics (Adams et al., 1998; Mortimer, 2004; Boschman et al., 2021a). The geology of New
202 Caledonia shares broad similarities with that of New Zealand: The Boghen Terrane of New
203 Caledonia has been correlated to the Torlesse Complex of New Zealand; both Jurassic-
204 Cretaceous accretionary complexes, and the Teremba Terrane of New Caledonia to the Murihiku
205 Terrane of New Zealand; both forearc terranes consisting of late Permian to Jurassic island-arc
206 derived strata (Cluzel and Meffre, 2002; Maurizot et al., 2020b). Cretaceous sedimentary
207 sequences that overlie the Torlesse accretionary complex from 100 Ma onwards in New Zealand
208 (Laird and Bradshaw, 2004; Crampton et al., 2019) provide important arguments for
209 interpreting the end of subduction: they are widely seen as signaling a transition from a
210 subduction margin to a passive margin (e.g., Field and Uruski, 1997; Laird and Bradshaw, 2004;
211 Edbrooke, 2017; Crampton et al., 1999; 2019). However, others have considered these Late
212 Cretaceous sequences to be accretionary shelf and slope basin fill that accumulated during
213 outbuilding of the accretionary wedge and that subduction continued until c. 84 Ma (Mazengarb
214 and Harris, 1994; Kamp, 1999; 2000; Gardiner and Hall, 2021). Deposition of subduction-
215 related volcanoclastic greywackes continued until c. 90 Ma in New Caledonia (Cluzel et al., 2010;
216 Maurizot et al., 2020b)

217 The oceanic lithosphere of the modern Pacific Plate contains three prominent oceanic
218 plateaus interpreted to have formed as a single ~120 Ma Large Igneous Province (LIP): the
219 conceptual Ontong Java Nui LIP (Taylor, 2006; Chandler et al., 2012). The three oceanic plateaus
220 that are thought to have once formed as Ontong Java Nui are currently separated by post-120
221 Ma Cretaceous oceanic basins. These oceanic plateaus are the Ontong Java Plateau, located to
222 the north of the Solomon Islands; the Manihiki Plateau, located to the northeast of Samoa; and
223 the Hikurangi Plateau, located offshore the North Island of New Zealand (Fig. 1). The Manihiki
224 Plateau is separated from the Ontong Java Plateau by the Ellice Basin, and the Hikurangi Plateau
225 is separated from the Manihiki Plateau by the Osbourn Trough (Fig. 1).

226

227 **3. Reconstruction approach, plate circuits, and reference frames**

228 Quantitative constraints on the convergence history between the plates of the
229 Panthalassa realm and the Zealandia margin of East Gondwana follows from the kinematic
230 reconstruction of the South Pacific region. The reconstruction presented here includes a
231 compilation of the most recent kinematic data and the new Pacific reference frame of Torsvik et
232 al. (2019). For the analysis in this paper, we focus on the history of the South Pacific region back
233 to the Early Cretaceous. Our reconstruction is made in GPlates, a freely available plate
234 reconstruction software (www.gplates.org; Boyden et al., 2011; Müller et al., 2018).

235 We restore spreading along the different mid-ocean ridges that existed in the southern
236 Panthalassa realm based on published marine magnetic anomaly data of ocean floor presently
237 underlying the south Pacific Ocean (Fig. 4), reviewed in section 4. The ages of the polarity
238 chrons in our reconstruction are updated to the timescale of Ogg (2020). We incorporate all
239 rotation poles as published, even though on short time intervals (<1 Myr) these are likely
240 subject to some noise (Iaffaldano et al., 2012). Our conclusions, however, are not affected by the
241 short time-scale noise and we prefer to see the effect of all interpreted isochrons rather than an
242 arbitrary selection of these.

243 In the absence of polarity reversals during the Cretaceous Normal Superchron (121.4-
244 83.7 Ma), the restoration of oceanic basins for this time interval is based on previously
245 published radiometric data from dredged and cored samples as well as published
246 interpretations of seafloor fabric (Fig. 4; see section 4). Magnetic anomaly picks and fracture
247 zone data were obtained from the Global Seafloor Fabric and Magnetic Lineation (GSFML)
248 Database (Matthews et al., 2011; Seton et al., 2014; Wessel et al., 2015). We restore intra-
249 continental deformation within East Gondwana applying a reconstruction hierarchy that uses
250 quantitative kinematic constraints on continental extension, transform motion, or crustal
251 shortening (see Boschman et al., 2014 and Van de Lagemaat et al., 2018a for details).

252 Plate convergence can best be quantified when a plate circuit is present that connects
253 the two converging plates through a series of active or fossil spreading ridges (Cox and Hart
254 1986). For times after the formation of the Pacific-Antarctic Ridge (Chron C34y, c. 83.7 Ma; see
255 section 4), plate convergence in the region can be reconstructed through a plate circuit that
256 constrains the motion of the Australian Plate relative to the Antarctic Plate based on the record
257 of oceanic spreading at the Southeast Indian Ridge (SEIR), and the motion of the Pacific Plate
258 relative to the Antarctic Plate by restoring spreading at the Pacific-Antarctic Ridge (PAR) (Fig.
259 5). The Late Cretaceous and Cenozoic opening of marginal and back-arc basins east of Australia
260 are reconstructed relative to the Australian Plate, that adds Zealandia-Australia, and Tonga-
261 Kermadec-Hikurangi trench-Zealandia motion to the plate circuit. In addition, the relative
262 motion of oceanic plates flooring the Pacific Ocean are reconstructed relative to the Pacific Plate
263 (Fig. 5). For the period of activity of the New Caledonia subduction zone in Paleocene to
264 Oligocene time, it is not possible to quantify partitioning of convergence over the Tonga and
265 New Caledonia trenches – only net convergence between Zealandia and the Panthalassa plates
266 can be quantified (Van de Lagemaat et al., 2018a). However, for the interval of interest of this
267 paper, this problem is of no consequence.

268 For times after the Cretaceous Normal Superchron, i.e. at C34y (post-83.7 Ma), we use
269 the ‘Antarctic’ plate circuit Zealandia – Australia – East Antarctica – West Antarctica – Pacific
270 (Fig. 5). Due to uncertainties in relative motion between West Antarctica and East Antarctica

271 before 45 Ma, some studies use a plate circuit for these times that ties the Lord Howe Rise to the
272 Pacific Plate directly before c. 45 Ma instead (i.e., the Australian circuit) using magnetic
273 anomalies in the Tasman Sea basin (e.g., Steinberger et al., 2004; Torsvik et al., 2019). In the
274 Australian circuit it is assumed that there is no plate boundary between the Pacific Plate and
275 Zealandia between 83 and 45 Ma. However, geological data from New Caledonia provides
276 evidence for the existence of a subduction zone between the Pacific Plate and the Norfolk Ridge
277 between c. 60 and 30 Ma (e.g. Cluzel et al., 2012; Van de Lagemaat et al., 2018a; Maurizot et al.,
278 2020b), which means that the Pacific Plate should not be reconstructed relative to Zealandia
279 after 60 Ma. Combined with recently improved constraints on deformation within Antarctica
280 (e.g. Granot et al., 2013; Granot and Dymant, 2018) leads us to prefer the Antarctic circuit for
281 our reconstruction, similar to Seton et al. (2012), Matthews et al. (2015), and Müller et al.
282 (2019). There is a c. 150 km difference in location of the Pacific relative to the Gondwana plates
283 between the Antarctic and Australian circuits at chron C34y (83.7 Ma).

284 Before the onset of Pacific-Antarctic Ridge spreading, the plate circuit is broken, as the
285 Panthalassa and Gondwana plates are connected through a subduction zone only (Seton et al.,
286 2012; Wright et al., 2016). The reconstruction of pre-chron C34y (83.7 Ma) relative motions
287 across the East Gondwana margin then relies on placing the Gondwana continents and the
288 Panthalassa plates in mantle reference frames that were developed for each of the two systems
289 separately (Fig. 5). For this reason, we put our reconstruction in a mantle reference frame for
290 the entire reconstruction period. The Gondwana continents are part of the Indo-Atlantic realm,
291 whose relative motions are constrained by the reconstruction of the Indian and Atlantic Oceans.
292 Several mantle reference frames are available for the Indo-Atlantic realm, from different
293 approaches and iterations. We will illustrate the sensitivity of the choice of reference frame for
294 convergence across the Zealandia margin, using the moving hotspot reference frames of O'Neill
295 et al. (2005), Torsvik et al. (2008), and Doubrovine et al. (2012), and the semi-quantitative slab-
296 fitted reference frame of Van der Meer et al. (2010). These reference frames are given in African
297 coordinates, requiring reconstructing the eastern Gondwana continents circuit to the African
298 Plate. For the period after the Cretaceous Normal Superchron, we also use the Indo-Atlantic
299 reference frame for the Panthalassa domain, as it is connected to the plate circuit. For the period
300 before chron C34y (83.7 Ma), when the plate circuit is broken, we use the Pacific reference
301 frame of Torsvik et al. (2019), who updated a fixed hotspot frame that constrains absolute
302 Pacific Plate motion back to 150 Ma. We incorporate the 'Earthbyte Model R' of Torsvik et al.
303 (2019), which corresponds to the Antarctic circuit as explained above.

304

305 **4. Review of kinematic data**

306 **4.1. Post-Cretaceous Quiet Zone plate reconstruction of ocean basins, and East**
307 **Gondwana fit**

308 The onset of spreading at the Pacific-Antarctic Ridge marks a major break in the plate
309 tectonic history of the Panthalassa-Pacific realm, as it formed the first passive margin that
310 connected the oceanic domain to the Indo-Atlantic plates after hundreds of millions of years
311 (e.g., Molnar et al., 1975; Seton et al., 2012; Wright et al., 2016 Müller et al., 2019). The oldest
312 magnetic anomaly that records spreading between the Campbell Plateau and Marie Byrd Land
313 (West Antarctica) is chron C33 (79.9 Ma; Wobbe et al., 2012), the oldest crust having formed
314 after the end of chron C34y, i.e., after 83.7 Ma. Farther east, however, the marine magnetic
315 anomaly of chron C34y (83.7 Ma) was identified just south of Chatham Rise and its conjugate
316 margin off the coast of Thurston Island (Larter et al., 2002; Eagles et al., 2004a; Wobbe et al.,
317 2012). There is no evidence for the existence of a plate boundary between the oceanic crust that
318 formed south of the Chatham Rise and the Campbell Plateau and oceanic crust of the Pacific
319 Plate, and it is therefore assumed that the Chatham Rise and Campbell Plateau have been part of
320 the Pacific Plate since the formation of the Pacific-Antarctic Ridge (Molnar et al., 1975;
321 Luyendyk, 1995). The set of marine magnetic anomalies of chron C34y (83.7 Ma) that formed
322 south of Chatham Rise and off the coast of Thurston Island is therefore the oldest marine
323 magnetic anomaly constraint for Pacific-West Antarctica spreading (Wobbe et al., 2012; Wright
324 et al., 2016). As these marine magnetic anomalies are located close to the continental margins of
325 Chatham Rise and West Antarctica, it is thought that true seafloor spreading started shortly
326 before the end of the Cretaceous Quiet Zone (Wobbe et al., 2012). Based on the extrapolation of
327 seafloor spreading rates, Wobbe et al. (2012) suggested that the first oceanic crust between
328 Chatham Rise and Thurston Island (West Antarctica) formed around 84 Ma, which is in accord
329 with the minimum age for the oceanic crust between Chatham Rise and West Antarctica, based
330 on a 83.9 ± 0.1 Ma Ar/Ar age of K-feldspar in a trachyte sample from Erik Seamount (Mortimer
331 et al., 2019), while rifting is thought to have started around 89 Ma (Wobbe et al., 2012). The
332 oldest oceanic crust between Chatham Rise and West Antarctica may have formed during
333 extension in the Bounty Trough (between 92 and 84 Ma; Grobys et al., 2008), before Chatham
334 Rise was captured by the Pacific Plate. The timing of the capture of Chatham Rise by the Pacific
335 remains uncertain, although it must have occurred in the 90-83.7 Ma interval: the location of the
336 Pacific Plate is constrained at either end of this time interval: 90 Ma is the youngest age in the
337 Pacific hotspot reference frame of Torsvik et al. (2019) and 83.7 Ma (i.e., chron C34y) is the
338 oldest marine magnetic anomaly constraint (Wright et al., 2016). Between those times (90-83.7
339 Ma), the Pacific Plate may have started to diverge from West Antarctica, but we reconstruct the
340 start of Pacific-Antarctic spreading based on the oldest marine magnetic anomaly constraint
341 (i.e., C34y; 83.7 Ma; Wobbe et al., 2012), similar to other reconstructions (e.g., Seton et al., 2012;

342 Wright et al., 2016; Müller et al., 2019). Any extension in the region (i.e., between Chatham Rise
343 and Campbell Plateau and West Antarctica) before that time is considered to not have involved
344 the Pacific Plate (Fig. 6D and Fig. 7C). We reconstruct the motion between the Pacific Plate and
345 West Antarctica using finite rotation poles of Croon et al. (2008) (present-C20; 43.5 Ma) and
346 Wright et al. (2016) (C21-C34y; 47.8-83.7 Ma). This is similar to the reconstruction of Müller et
347 al. (2019), although we incorporate all published rotation poles whereas Müller et al. (2019)
348 only used rotation poles for selected polarity chrons.

349 Shortly before the start of chron C33 (79.9 Ma) a piece of lithosphere broke off of West
350 Antarctica to form the Bellingshausen Plate (Stock and Molnar, 1987). The Bellingshausen Plate
351 started to rotate clockwise relative to West Antarctica and acted as an independent plate until
352 chron C27 (62.5 Ma; Stock and Molnar, 1987; Cande et al., 1995; Eagles et al., 2004b; Wobbe et
353 al., 2012; Wright et al., 2016). During this time window, the northern margin of the
354 Bellingshausen Plate was formed by a spreading ridge with the Pacific Plate and its western
355 margin was defined by a short transform margin with the Marie Byrd Land sector of West
356 Antarctica, close to the Euler pole of Bellingshausen-West Antarctica motion (Wright et al.,
357 2016). To the east, the Bellingshausen Plate was bounded by a right-lateral transform fault from
358 the Aluk Plate (Larter et al., 2002; Eagles et al., 2004). To the south, the Bellingshausen Plate
359 was converging with the Thurston Island sector of West Antarctica, although the maximum total
360 amount of convergence was less than 250 km and no mature subduction zone developed
361 (Wright et al., 2016). Like the reconstruction of Müller et al. (2019), we reconstruct the 79.9-
362 62.5 Ma motion of the Bellingshausen Plate relative to the Pacific Plate using the finite rotation
363 poles of Wright et al. (2016), which are based on marine magnetic anomalies of chrons C33-C27.

364 We tentatively suggest that friction at the transform fault that formed the eastern plate
365 boundary of the West Antarctic Plate (Heezen Fracture Zone) led to the partial coupling of West
366 Antarctica with the Aluk Plate. After the formation of the Pacific-Antarctic ridge, the Pacific-
367 West Antarctica spreading and Pacific-Aluk spreading ridges were parallel, but Pacific-Aluk
368 spreading occurred at a higher rate (~3.5 and ~7 cm/yr half-spreading rate, respectively). This
369 resulted in lengthening of the transform fault that formed the plate boundary between the West
370 Antarctic and Aluk plates. The partial coupling of part of West Antarctica with Aluk caused the
371 formation of the Bellingshausen Plate, which was being dragged along by the Aluk Plate. This
372 dragging resulted in clockwise rotation of Bellingshausen relative to West Antarctica. This
373 suggestion is similar to what was proposed by Eagles et al. (2004b), who also suggested that the
374 independent motion of Bellingshausen was related to the lengthening of the West Antarctica-
375 Pacific transform plate boundary. A similar process was responsible for the formation of e.g. the
376 Bauer microplate, which moved independently between c. 18-6 Ma, partitioning strain between
377 the Pacific and Nazca plates (Eakins and Lonsdale, 2003).

378 Before C34y (83.7 Ma), pre-drift extension had already started to separate the Campbell
379 Plateau from Marie Byrd Land and Chatham Rise from the Campbell Plateau (Molnar et al.,
380 1975; Stock and Cande, 2002; Riefstahl et al., 2020) (Fig. 6D and 7C). We reconstruct c. 180 km
381 of pre-drift extension between the Campbell Plateau and Marie Byrd Land between 95 and 83.7
382 Ma, based on the estimated 90 km of extension in both margins based on crustal thickness
383 calculations (Wobbe et al., 2012). We reconstruct c. 200 km of extension in the Bounty Trough
384 (between Chatham Rise and the Campbell Plateau) between 92 and 84 Ma, based on the
385 reconstruction derived from crustal thickness calculations of Grobys et al. (2008). This
386 reconstruction also leads to extension between Chatham Rise and the Thurston Island sector of
387 West Antarctica, where plate boundary activity may have started around 89 Ma (Wobbe et al.,
388 2012).

389 A long-lived volcanic arc and accretionary prism on the Antarctic Peninsula shows that
390 subduction continued throughout the Mesozoic and Cenozoic until the present-day (e.g., Burton-
391 Johnson and Riley, 2015; Jordan et al., 2020). The plate that is subducting below the Antarctic
392 Peninsula, the Aluk Plate, is therefore thought to be a descendent of the Phoenix Plate (Fig. 1;
393 e.g., Barker, 1982; Eagles, 2004). Interestingly, however, for much of the Cenozoic, and until the
394 cessation of spreading around 3.3 Ma, the Aluk Plate has not been spreading relative to the
395 Pacific Plate, but relative to oceanic lithosphere of West Antarctica (Eagles, 2004). Marine
396 magnetic anomalies that formed along the Aluk-West Antarctica Ridge are preserved on the
397 Aluk Plate back to C6A (21.32 Ma; Larter and Barker, 1991; Eagles, 2004), and on conjugate
398 West Antarctica oceanic lithosphere back to C27 (62.52 Ma) (Cande et al., 1982). To the
399 northwest, West Antarctica also contains a set of magnetic anomalies from C21 (47.8 Ma) and
400 younger that record spreading between West Antarctica and the Pacific Plate (Cande et al.,
401 1982; Cande et al., 1995; Croon et al., 2008). This spreading was near-parallel to West
402 Antarctica-Aluk spreading, showing simultaneous and near-parallel spreading of West
403 Antarctica with both the Pacific and Aluk plates (Wright et al., 2016).

404 Around the time of chron C21 (c. 47 Ma), part of the Pacific Plate that formed through
405 Pacific-Aluk spreading was captured by the West Antarctic Plate (Cande et al., 1982; McCarron
406 and Larter, 1998; Eagles et al., 2004a). Shortly before capture, the transform plate boundary
407 between the West Antarctic and Pacific plates was lengthening due to the higher Pacific-Aluk
408 compared to Pacific-West Antarctic spreading rates, similar to the situation that resulted in the
409 formation of the Bellingshausen Plate. During capture, the Pacific-Antarctic ridge propagated
410 into oceanic crust of the Pacific Plate that formed around C27 (c. 62.5 Ma) (Cande et al., 1982).
411 At the southern end of the captured crust, the Pacific-Aluk ridge was replaced by the West
412 Antarctic-Aluk ridge.

413 To the northeast, West Antarctica shared a spreading ridge with the Farallon Plate and
414 its daughter Nazca Plate (Fig. 6H-J) (Wright et al., 2016). However, before C21 (47.3 Ma), there
415 was no Antarctic oceanic crust that separated the Aluk Plate from the Pacific Plate (Fig. 6G):
416 instead, the Aluk Plate was spreading directly with the Pacific Plate, recorded by marine
417 magnetic anomalies back to C34y (83.7 Ma) on the Pacific Plate (Cande et al., 1982; Cande et al.,
418 1995; Larter et al., 2002; Eagles et al., 2004a; Croon et al., 2008). In our reconstruction we use
419 rotation poles of Aluk-West Antarctica and Aluk-Pacific motion back to C34y (83.7 Ma) of Eagles
420 (2004), Eagles and Scott (2014) and Wright et al. (2016), similar to Müller et al. (2019). The
421 tectonic history of the Aluk Plate prior to C34y (83.7 Ma) cannot be constrained by magnetic
422 anomalies due to the Cretaceous Quiet Zone.

423 In the East Pacific, the Nazca Plate is spreading along the East Pacific Rise from the
424 Pacific Plate and along the Chile Ridge from West Antarctica, while subducting below South
425 America (Fig. 1). The Nazca Plate formed c. 22 Ma (chron C6B), as the southern remnant of the
426 broken up Farallon Plate (Barckhausen et al., 2001; 2008; Wright et al., 2016). The East Pacific
427 Rise records spreading between the Pacific and Nazca plates (and its predecessor the Farallon
428 Plate) back to chron C23 (51.7 Ma) on the Nazca Plate (older magnetic anomalies have been lost
429 to subduction below South America) and back to chron C34y (83.7 Ma) on the Pacific Plate
430 (Atwater and Severinghaus, 1989; Barckhausen et al., 2008; Wilder, 2003; Handschumacher et
431 al., 1976). Spreading between the Nazca Plate and West Antarctica is recorded at the Chile Ridge
432 back to chron C24 (53.9 Ma) on West Antarctica and back to chron C5E (18.5 Ma) on the Nazca
433 Plate (Cande et al., 1982; Tebbens et al., 1997). We reconstruct the Nazca Plate relative to the
434 Pacific Plate, using the finite rotation poles based on marine magnetic anomalies back to chron
435 C6B (22.3 Ma) of Tebbens and Cande (1997), as published in Wright et al. (2016), similar to
436 Müller et al. (2019). We include the Bauer Microplate that formed in Miocene times at the
437 Nazca-Pacific ridge using magnetic anomalies C5E-C3A (18.5-6.7 Ma) identified by Eakins and
438 Lonsdale (2003), with rotations computed in GPlates. We do not include the Galapagos, Easter
439 and Juan Fernandez microplates in our reconstruction, which formed about 5 Ma (Tebbens and
440 Cande, 1997; Wright et al., 2016). The Farallon Plate is reconstructed relative to the Pacific Plate
441 between 22.3 (chron C6B) and 83.7 Ma (chron C34y) using the finite rotations poles of Wright
442 et al. (2016), like in Müller et al. (2019). The record of Farallon-Pacific spreading during and
443 before the Cretaceous Quiet Zone will be discussed in section 4.2.

444 Cenozoic relative motion between East Antarctica and West Antarctica is constrained by
445 marine magnetic anomalies that formed in the Adare and Northern basins between chrons C5
446 and C27 (11.1-62.5 Ma) (Cande and Stock, 2004; Granot et al., 2013; Granot and Dyment, 2018).
447 We incorporate the finite rotation poles of Granot and Dyment (2018), Granot et al. (2013), and
448 Cande and Stock (2004) for chrons C5-C8, C12-C18, and C20-C27, respectively. Mesozoic

449 extension in the West Antarctic Rift System (WARS) between West Antarctica and East
450 Antarctica is poorly constrained, but a main phase of extension was proposed to have occurred
451 in the mid-Late Cretaceous, based on low temperature geochronology studies (Lawver and
452 Gahagan, 1994; Fitzgerald, 2002; Spiegel et al., 2016; Veevers, 2012). Based on crustal thickness
453 estimates (An et al., 2015; Llubes et al., 2018; Shen et al., 2018), we reconstruct c. 100 km of
454 extension in the West Antarctic Rift System between 95 and 84 Ma (Fig. 7).

455 Australia-East Antarctica motion is based on marine magnetic anomalies back to chron
456 C34y (83.7 Ma), although seafloor spreading was slow before chron C17o (~38 Ma) (Cande and
457 Stock, 2004b; Whittaker et al., 2007; 2013). Pre-drift extension between East Antarctica and
458 Australia started at 136 Ma (Whittaker et al., 2013), and we base the East Gondwana fit of East
459 Antarctica and Australia on the reconstruction of the extended conjugate continental margins of
460 Williams et al. (2011) and Gibbons et al. (2012). Our Australia-East Antarctica reconstruction is
461 similar to that of Müller et al. (2019).

462 The Late Cretaceous to early Eocene separation of Lord Howe Rise (North Zealandia)
463 from Australia is recorded by marine magnetic anomalies C24-C34y (53.9-83.7 Ma) in the
464 Tasman Sea (Gaina et al., 1998). We use the finite rotation poles of Gaina et al. (1998) in our
465 reconstruction, like Seton et al. (2012) and Müller et al. (2019). Pre-drift extension is thought to
466 have started c. 95 Ma, concurrently with extension in the New Caledonia Basin, between the
467 Norfolk Ridge and Lord Howe Rise (Fig. 6D-E and 7C) (Grobys et al., 2008). The back-arc basins
468 between Lord How Rise and the Tonga-Kermadec-Hikurangi subduction zone are reconstructed
469 as in Van de Lagemaat et al. (2018a), using marine magnetic anomaly constraints from Yan and
470 Kroenke (1993), Sdrolias et al. (2003), and Herzer et al. (2011).

471 We connect the plate circuit of our reconstruction to Africa by reconstructing East
472 Antarctica-Africa motion through the South Atlantic Ocean. This is based on finite rotation poles
473 based on marine magnetic anomalies back to chron M38 (c. 164 Ma) of DeMets et al. (2021) (C1-
474 C23; 0-51.7 Ma), Cande et al. (2010) (C23-C29; 51.7-64.9 Ma), Bernard et al. (2005) (C29-C33;
475 64.9-79.9 Ma), and Mueller and Jokat (2019) (C34y-M38; 84.7-162.9 Ma).

476

477 **4.2. Pre-C34y plate reconstruction of the Paleo-Pacific realm**

478 **4.2.1. Evolution of the Phoenix Plate**

479 Direct kinematic constraints on the evolution of the Phoenix Plate come from marine
480 magnetic anomalies preserved on the Pacific Plate (Nakanishi et al., 1992). The oldest of these
481 anomalies, preserved in the west Pacific Ocean, formed at the Pacific-Phoenix Ridge (Larson and
482 Chase, 1972), and were identified as M29n.2n – M1n (Nakanishi et al., 1992), indicating that
483 Pacific-Phoenix spreading was active from at least 155.9 to 123.8 Ma. We reconstruct the
484 motion of Phoenix for this time interval using GPlates, by mirroring the marine magnetic

485 anomalies that are preserved on the Pacific Plate, assuming symmetric spreading (Fig. 6A-B).
486 We reconstruct Pacific-Phoenix spreading until 120 Ma, the timing of Ontong Java Nui break-up
487 (see section 4.2.2) (Taylor, 2006; Chandler et al., 2012).

488 While Pacific-Phoenix spreading was active, the Pacific Plate was also spreading with the
489 Farallon and Izanagi plates (or Izanami Plate; see Boschman et al., 2021b). Marine magnetic
490 anomalies that formed during chrons M29 – M0 (156.9-121.4 Ma) were identified on the
491 eastern side of the Pacific triangle (Nakanishi et al., 1992), which constrain spreading between
492 the Pacific and Farallon plates. Pacific-Izanagi spreading is constrained by marine magnetic
493 anomalies that formed during chrons M35 – M5 (160.9-127.5 Ma) (Nakanishi et al., 1992). We
494 reconstruct Farallon-Pacific and Izanagi-Pacific spreading in this time interval based on the
495 marine magnetic anomalies (Nakanishi et al., 1992), using the reconstruction poles of Boschman
496 et al. (2021a).

497 Marine magnetic anomalies that formed in the southeast corner of the Pacific triangle
498 suggest the formation of two microplates (the Trinidad and Magellan microplates) around the
499 Pacific-Farallon-Phoenix triple junction (Nakanishi and Winterer, 1998). The Trinidad
500 microplate formed around chron M21 (146.6 Ma) and stopped acting as a separate plate around
501 chron M14 (136.9 Ma) (Nakanishi and Winterer, 1998). The Magellan microplate formed
502 around chron M15 (138.5 Ma) and remained active until chron M9 (129.9 Ma), when it merged
503 with the Pacific Plate (Nakanishi and Winterer, 1998). We incorporate the independent motion
504 of the Magellan microplate between chrons M15 and M9 (138.5 – 129.9 Ma) in the
505 reconstruction. We computed finite rotation poles for this reconstruction in GPlates, based on
506 the magnetic anomaly picks of Nakanishi and Winterer (1998). We do not reconstruct the
507 Trinidad microplate, because there are not enough marine magnetic anomaly identifications for
508 a reliable reconstruction of this microplate.

509 From reconstruction of Pacific-Farallon and Pacific-Izanagi spreading, it follows that the
510 Phoenix Plate also formed mid-oceanic ridges with the Farallon and Izanagi plates (Fig. 6A). The
511 location of these spreading ridges relative to the Pacific triangle is unknown, but undated
512 marine magnetic anomalies in the Caribbean plate have orientations that are consistent in
513 direction with those that would have formed at the Farallon-Phoenix ridge, and ages of ocean
514 floor exposed in western Costa Rica are consistent with a Jurassic age of spreading of this
515 lithosphere (Boschman et al., 2019). This suggests that prior to the Cretaceous Quiet Zone, the
516 Farallon-Phoenix ridge was located at the longitude of (and subducting below) northern South
517 America. The Izanagi-Phoenix ridge is generally assumed to have remained north of Australia
518 (e.g. Seton et al., 2012). The Phoenix Plate and its Cretaceous to Cenozoic daughters were
519 therefore lost along a continuous subduction margin that spanned from the Caribbean region,

520 down along the westcoast of South America, continuing along the West Antarctic and Zealandia
521 margins to northeast Australia and possibly into Southeast Asia (Fig. 2 and 6A).

522

523 **4.2.2. Ontong Java Nui break-up**

524 The Phoenix lineations on the Pacific Plate are overlain in the west by the Ontong Java
525 Plateau (Larson, 1997). South of the Phoenix lineations is the oceanic Ellice Basin, which is
526 devoid of marine magnetic anomalies due to its formation during the Cretaceous Normal
527 Superchron, but has east-west trending fracture zones (Benyshek et al., 2019). According to the
528 'superplateau' hypothesis, the Ontong Java Plateau, together with the Manihiki and Hikurangi
529 plateaus was emplaced as a single Large Igneous Province, known as Ontong Java Nui, around
530 125-120 Ma (Fig. 6B; Taylor, 2006; Chandler et al., 2012). Shortly after emplacement, Ontong
531 Java Nui broke up into the three modern plateaus through spreading in the Ellice Basin and
532 Osbourn Trough (Taylor, 2006; Chandler et al., 2012; Hochmuth et al., 2015). The Ontong Java
533 Nui LIP erupted on either side of the already existing Pacific-Phoenix spreading ridge: the
534 Ontong Java Plateau represents the part of the LIP that formed on the Pacific Plate, whereas the
535 Manihiki and Hikurangi plateaus formed on the former Phoenix Plate (Larson, 1997; Seton et al.,
536 2012). After separation, the Manihiki and Hikurangi plateaus became part of independent
537 tectonic plates, which grew larger than the original LIPs through the formation of new oceanic
538 crust at their bounding mid-ocean ridges (Fig. 6B-C) (Seton et al., 2012). We refer to these
539 plates as the Manihiki and Hikurangi plates. When we discuss the actual LIPs, we will refer to
540 them as Manihiki and Hikurangi plateaus. Restoration of spreading in the Ellice Basin and
541 Osbourn Trough reconstructs the Hikurangi Plate via the Manihiki Plate relative to the Pacific.
542 The emplacement and subsequent break-up of Ontong Java Nui also resulted in the
543 fragmentation of the Phoenix Plate (e.g. Seton et al., 2012). The spreading history of the Ellice
544 Basin and Osbourn Trough is thus of key importance in the search of the Phoenix Plate and for
545 reconstructing the convergence history between the Pacific realm plates and the Zealandia
546 margin of East Gondwana.

547 The Ontong Java Nui fit of the three plateaus is based on the interpretation of conjugate
548 rifted margins (Taylor, 2006; Chandler et al., 2012). The general absence of marine magnetic
549 anomalies in the Cretaceous Quiet Zone makes the opening history of these basins challenging
550 to reconstruct in detail. The start of opening of the basins postdated the main formation phase
551 of Ontong Java Nui, which occurred at 125 – 120 Ma. This age is based on $^{40}\text{Ar}/^{39}\text{Ar}$ dating of
552 tholeiitic basalts dredged from the three plateaus (Mahoney et al., 1993; Hoernle et al., 2010;
553 Timm et al., 2011) and on the age of sediments directly overlying pillow basalts (Winterer et al.,
554 1974; Sliter et al., 1992). Spreading at the Osbourn Trough started before 115 Ma, based on 115
555 ± 1 Ma U-Pb zircon ages from dredged lavas and volcanoclastic sandstones from the West

556 Wishbone Ridge (Mortimer et al., 2006). Dating of rift-related structures revealed a c. 120 Ma
557 age of separation between the Hikurangi and Manihiki plateaus (Davy et al., 2008). The onset of
558 rifting in the Ellice Basin between the Manihiki and Ontong Java plateaus is thought to have
559 occurred concurrently with the onset of spreading at the Osbourn Trough, although this is not
560 confirmed by radiometrically dated dredge samples (e.g., Chandler et al., 2012; Hochmuth et al.,
561 2015).

562 A tectonic reconstruction for the final stages of opening of the Ellice Basin was
563 presented by Benyshek et al. (2019), based on detailed bathymetric data from the center of the
564 basin. They tentatively suggested ages for their rotation poles, based on estimated spreading
565 rates, but these await confirmation by radiometric dating of basement samples (Benyshek et al.,
566 2019). The end of spreading in the Ellice Basin most likely occurred before the end of the CNS,
567 i.e., before 83.7 Ma.

568 Because no marine magnetic anomalies have been confidently identified, spreading at
569 the Osbourn Trough is also widely interpreted to have occurred entirely during the Cretaceous
570 Normal Superchron (e.g., Chandler et al., 2012). The age of arrest of the Osbourn Trough
571 opening is important for the age of cessation of subduction at the Gondwana margin of New
572 Zealand. The age of 86 Ma incorporated in the widely used global plate models (Seton et al.,
573 2012; Matthews et al., 2016; Muller et al., 2019) came from Worthington et al. (2006), who
574 interpreted the age of arrest of spreading from an age for arrest of subduction based on
575 geological interpretations from New Zealand: occurrence of calc-alkaline volcanism until 89 Ma
576 (Smith and Cole, 1997), the interpreted ongoing outbuilding of an accretionary wedge
577 (Mazengarb and Harris, 1994; Kamp, 1999; 2000) and an 86 Ma episode of metamorphism (Vry
578 et al., 2004), all recognized in New Zealand. But because this young age of subduction arrest is
579 widely disputed by the geological community of New Zealand who prefer a 105-100 Ma (e.g.,
580 Bradshaw, 1989; Luyendyk, 1995; Crampton et al., 2019; Mortimer et al., 2019; Gardiner et al.,
581 2021), and it is this debate that we aim to reconcile, our reconstruction of Osbourn Trough
582 should remain independent from the interpretations of the geology of New Zealand. Billen and
583 Stock (2000) tentatively identified anomalies C33 and C32 (79.9 and 73.6 Ma) in the Osbourn
584 Trough. Because the magnetic anomalies are not obvious lineations, they called for more
585 magnetic data and dredge samples. The magnetic anomalies have thus far not been
586 independently confirmed, but Mortimer et al. (2019) reported an 84.4 ± 3.5 Ma $^{40}\text{Ar}/^{39}\text{Ar}$ age of
587 plagioclase in a basalt flow recovered from bore hole DSDP595, which is located c. 200 km north
588 of the former Osbourn Trough spreading center (Fig. 4). Through extrapolation of spreading
589 rates, they proposed that Osbourn Trough spreading may have continued until ~ 79 Ma
590 (Mortimer et al., 2019), implying that spreading may indeed have continued after the
591 Cretaceous Quiet Zone as suggested by Billen and Stock (2000). However, the 84.4 Ma age is a

592 tentative age, as the effects of seawater alteration could not be entirely ruled out (Mortimer et
593 al., 2019). On the other hand, Zhang and Li (2016) suggested that spreading at the Osbourn
594 Trough ceased around 101 Ma, which would require ultrafast spreading rates of 19 cm/yr. This
595 is based on a 103.7 ± 2.3 Ma Re-Os isochron age of basalts recovered from bore hole U1365 (Fig.
596 4), adjacent to bore hole DSDP595, which contradicts the 84.4 Ar/Ar age of Mortimer et al.
597 (2019).

598 We reconstruct the start of spreading in both basins at 120 Ma (Fig. 6B), following
599 Chandler et al. (2012), similar to Seton et al. (2012) and Müller et al. (2019). For the Osbourn
600 Trough, we use rotation poles of Chandler et al. (2012) to reconstruct the spreading history, but
601 we incorporate the new constraints from Mortimer et al. (2019) of spreading until 79 Ma rather
602 than the contested, New Zealand geology-based 86 Ma estimate of Worthington et al. (2006)
603 that is used in Seton et al. (2012) and Müller et al. (2019). We note that the age for the end of
604 Osbourn Trough spreading may change in the future if more reliable radiometric dating of the
605 Osbourn Basin becomes available, and we will discuss below what difference a different age
606 would make for the estimate for subduction arrest at the New Zealand margin. For the Ellice
607 Basin, we use the Chandler et al. (2012) rotation pole for the Ontong Java-Manihiki fit at 120 Ma
608 and the rotation poles of Benyshek et al. (2019) for subsequent opening, with spreading ending
609 at 90 Ma.

610 The contemporaneous opening of the Ellice Basin and Osbourn Trough requires that a
611 mid-ocean ridge existed between the Hikurangi and Pacific plates (Fig. 6B-E). The rate and
612 direction of spreading along this ridge follows from the Pacific-Manihiki and Manihiki-
613 Hikurangi reconstructions. This spreading ridge, as well as the Pacific-Manihiki-Hikurangi triple
614 junction was lost to subduction at the Tonga-Kermadec-Hikurangi subduction zone during the
615 Cenozoic (Fig. 6E-J).

616

617 **4.2.3. Seafloor fabric**

618 To the east of the Manihiki and Hikurangi plates, Seton et al. (2012) identified two more
619 daughter plates of the Phoenix Plate: Chasca and Catequil. We continue using the name Chasca
620 Plate, but the Catequil Plate of Seton et al. (2012) is the same as the Aluk Plate in our
621 reconstruction. We prefer the name Aluk Plate, because it is the established name for the
622 remnant of this plate whose lithosphere remains in the southeast Pacific today. As with Seton et
623 al. (2012), we derive the former existence of the Chasca and Aluk plates from seafloor fabric and
624 marine magnetic anomaly identifications.

625 The pre-83.7 Ma existence of the Aluk Plate follows from trends in the seafloor fabric
626 east of the Osbourn Trough. The extinct Osbourn Trough spreading center can be followed
627 eastwards until longitude 165°W, where it suddenly stops (Fig. 8). North and south of the

628 Osbourn Trough abyssal hill trends are WNW-ESE for the older part of the basin, and E-W for
629 the youngest part (Downey et al., 2007, see also their Fig. 6). These abyssal hill trends, together
630 with NNE-SSW trending fracture zones constrains the NNE-SSW to N-S spreading direction of
631 the Hikurangi Plate relative to the Manihiki Plate. This trend in seafloor fabric that formed at the
632 Osbourn Trough is delineated by the NNE-SSW trending Manihiki Scarp and the West Wishbone
633 Ridge, clear traces in the ocean floor (Fig. 8). East of the Manihiki Scarp and West Wishbone
634 Ridge, abyssal hills are trending ENE-WSW (Downey et al., 2007, their Fig. 6) and fracture zones
635 are trending NNW-SSE (Fig. 8). This suggests that the oceanic crust here formed at a different
636 spreading center, between different plates (Downey et al., 2007). We suggest here that this part
637 of oceanic crust formed through spreading between the Manihiki and Aluk plates, both
638 daughters of the Phoenix Plate. There is no remnant of an extinct spreading ridge preserved in
639 this part of the Pacific Plate, which suggests that all oceanic crust preserved here formed as part
640 of the Manihiki Plate (e.g., Seton et al., 2012). As Manihiki was incorporated into the Pacific Plate
641 at c. 90 Ma (Benyshek et al., 2019), the Manihiki-Aluk ridge became the Pacific-Aluk ridge at this
642 time. The location of the Pacific-Aluk Ridge is constrained after 83.7 Ma by marine magnetic
643 anomalies preserved on the Pacific Plate (Fig. 4 and 6E; see also section 4.1) (Cande et al., 1995;
644 Larter et al., 2002; Eagles et al., 2004; Wobbe et al., 2012). The direction of spreading between
645 the Manihiki/Pacific and Aluk plates follows from the NNW-SSE directed fracture zones that are
646 preserved on the Pacific Plate (Fig. 8). The average rate of Manihiki-Aluk spreading follows from
647 the 120 Ma break-up configuration of the Phoenix Plate into these plates and the chron C34y
648 (83.7 Ma) location of the Aluk-Pacific ridge, which is constrained by marine magnetic anomalies
649 on the Pacific Plate (Larter et al., 2002; Eagles et al., 2004). We reconstruct a constant spreading
650 rate in this 120-83.7 Ma period.

651 The nature of the plate boundary between the Aluk and Hikurangi plates follows from
652 the reconstruction of the Hikurangi and Aluk plates relative to the Manihiki Plate. In our
653 reconstruction, Aluk-Manihiki spreading occurred at a higher rate than Hikurangi-Manihiki
654 spreading (~8.5 cm/yr and ~4.5 cm/yr half-spreading rate, respectively) (Fig. 6B-D). As a
655 result, between 120 and 110 Ma, the plate boundary between the Aluk and Hikurangi plates was
656 a right-lateral transform fault northeast of the Hikurangi Plateau, forming the West Wishbone
657 Ridge. After 110 Ma, some extension occurred between the Aluk and Hikurangi plates east of the
658 Hikurangi Plateau, accommodated by a mid-ocean ridge. South of the Hikurangi Plateau, the
659 plate boundary between the Hikurangi and Aluk plates was a mid-ocean ridge from 120 Ma
660 until its subduction below the Zealandia margin around 100-90 Ma (Fig. 6B-C and 7).

661 From the northeast corner of the Manihiki Plateau towards the south, there is a clear
662 trace in the seafloor fabric (Fig. 8). This feature has been identified as a trace of a former triple
663 junction (Larson and Chase, 1972), and was named the Tongareva triple junction (Larson et al.,

664 2002). It was previously suggested that the Tongareva triple junction formed the junction
665 between the Pacific, Farallon, and Phoenix plates (e.g., Larson et al., 2002; Viso et al., 2005;
666 Hochmuth and Gohl, 2017). We instead infer that the Tongareva triple junction formed the
667 junction between Manihiki, Chasca and Aluk plates, until c. 90 Ma, when Manihiki merged with
668 the Pacific Plate. Between 90 and 83.7 Ma, the Tongareva triple junction was the junction of the
669 Pacific, Chasca and Aluk plates, after which it became the triple junction between Pacific,
670 Farallon and Aluk plates when Chasca was captured by Farallon (Fig. 6B-F).

671 The existence of the Chasca Plate follows from rift structures on the northeast margin of
672 the Manihiki Plateau (Fig. 8) (Larson et al., 2002; Viso et al., 2005). It was previously suggested
673 that this fragment was incorporated into the Farallon Plate at 110 Ma (Hochmuth and Gohl,
674 2017). The location of the Farallon Plate relative to the Pacific Plate is constrained by marine
675 magnetic anomalies of chrons C34y (83.7) and M0 (121.4). Attaching a fragment of oceanic
676 crust that formed east of the Manihiki Plateau to the Farallon Plate at 110 Ma, however, leads to
677 convergence along the southeast margin of the Manihiki Plateau. This convergence is
678 contradicted by the existence of the Tongareva triple junction trace, as described above. Instead,
679 we reconstruct independent motion of the Chasca Plate until 83.7 Ma. The capture of the Chasca
680 Plate by the Farallon Plate, which resulted from the inactivation of the transform fault
681 (Clipperton Fracture Zone) that separated the Chasca and Farallon plates, may have occurred a
682 few millions of years earlier. This would require higher Chasca – Manihiki/Pacific spreading
683 rates, but these are unknown. We therefore choose to reconstruct the capture at the time of
684 C34y (83.7 Ma), as this marine magnetic anomaly provides the first positive evidence that the
685 Chasca plate was captured. Seton et al. (2012) and Chandler et al. (2012) incorporate the Chasca
686 Plate into the Farallon Plate a few million years earlier at 86 Ma, contemporaneous with the
687 cessation of Osborn Trough spreading in their model (see section 4.2.2).

688 We reconstruct the start of Chasca – Manihiki motion at 120 Ma, the same time as the
689 onset of spreading between the other daughters of the Phoenix Plate (Chandler et al., 2012).
690 Rotation poles of the Chasca Plate relative to the Manihiki Plate are calculated in GPlates. In our
691 reconstruction, we ensure that early motion of the Chasca Plate follows the trend of the curved
692 rift structures at the NE Manihiki margin (Fig. 8). In addition, we assume that the Pacific-
693 Farallon ridge at 83.7 Ma formed at the location of the Pacific-Chasca ridge, after Manihiki was
694 captured by the Pacific Plate at 90 Ma (Benyshek et al., 2019) and Chasca was captured by
695 Farallon.

696 The rotation poles for the reconstruction of the Ellice Basin include a rotation of the
697 Manihiki Plate relative to the Pacific Plate between 102 and 98 Ma, based on a change in
698 fracture zone orientation in the Ellice Basin from ~E-W to WNW-ESE (Taylor, 2006; Chandler et
699 al., 2012; Benyshek et al., 2019). As the Chasca Plate is reconstructed relative to the Manihiki

700 Plate in our plate circuit, the rotation modeled by Benyshek et al. (2019) also results in a
701 rotation of the Chasca Plate. This in turn leads to convergence at the Chasca-Farallon plate
702 boundary that at that time was still located at the latitude of northern South America. This
703 rotation of the Chasca Plate coincides with the estimated timing of subduction initiation at the
704 western Caribbean plate boundary of modern Central America (Whattam and Stern, 2015;
705 Boschman et al., 2019), which at 100 Ma was still located far west within the eastern
706 Panthalassa realm (e.g., Pindell and Kennan, 2009; Boschman et al., 2014). Rotation of the
707 Manihiki Plate may thus have resulted in subduction initiation at the future western Caribbean
708 plate boundary.

709

710 **5. Discussion**

711 The kinematic constraints reviewed in section 4 lead to a plate kinematic evolution from 150
712 Ma onward as portrayed in Fig. 6, and in snapshots highlighting the final stages of subduction in
713 Fig. 7. We provide GPlates reconstruction files and an animation of the reconstruction in the
714 supplementary information. Below, we discuss uncertainties in our reconstruction, offer
715 interpretations of possible dynamic drivers of plate reorganizations, and evaluate until when
716 convergence along the Gondwana margin must have continued. Finally, we discuss how
717 differences between plate kinematics and geology-based interpretations may be reconciled, and
718 what opportunities our reconstruction provides for future geological research.

719

720 **5.1 Dating the end of convergence across the Gondwana margins**

721 During the Paleozoic and Mesozoic, the vast Phoenix Plate occupied large parts of the
722 south Panthalassa Ocean. After the birth of the Pacific Plate around 190 Ma (Seton et al., 2012;
723 Boschman and Van Hinsbergen, 2016), the Phoenix Plate formed spreading ridges with the
724 Pacific, Izanagi/Izanami and Farallon plates. Subduction at the Gondwana margin of South
725 America, Antarctica, and Australia/Zealandia is not controversial, although more plates may
726 have been involved between the Phoenix Plate and the Gondwana margin (e.g., Boschman et al.,
727 2021a). Our reconstruction from 150 Ma until the 125-120 Ma emplacement of the Ontong Java
728 Nui LIP, placed in the Pacific hotspot reference frame of Torsvik et al. (2019) and the Indo-
729 Atlantic slab-fitted frame of Van der Meer et al. (2010) straightforwardly shows convergence of
730 Phoenix in the west, south, and east, consistent with geological records from South America,
731 Antarctica, and Zealandia (Mortimer et al., 2014; Burton-Johnson and Riley, 2015; Pepper et al.,
732 2016; Jordan et al., 2020; Maurizot et al., 2020b). Along the eastern margin of the southern
733 Pacific, convergence and subduction continue today (Fig. 1). Conversely, convergence ceased
734 along the southern and western margins in the Late Cretaceous, which was followed by re-
735 initiation of subduction in the west during the Cenozoic (e.g. Seton et al., 2012; Van de Lagemaat

736 et al., 2018a). In this section, we establish until when, according to plate kinematic constraints,
737 subduction continued. In addition, we examine whether the choice of mantle reference frame is
738 of influence on this age estimation.

739 It is well agreed upon that a subduction zone was present along the entire East
740 Gondwana margin, from the Antarctic Peninsula to New Caledonia, until 105 Ma (Bradshaw,
741 1989; Luyendyk, 1995; Maurizot et al., 2020b; Gardiner et al., 2021). In addition, our plate
742 reconstruction shows that convergence at the Zealandia and Antarctic margins continued, until
743 at least 90 Ma and possibly until 85 Ma (Fig. 9). This is well beyond 105-100 Ma, when some
744 models that are based on onshore geology (e.g., the onset of continental extension and the
745 change in geochemistry of magmatism) argue for the cessation of subduction along the
746 Zealandia sector of East Gondwana (Bradshaw, 1989; Davy et al., 2008; Crampton et al., 2019;
747 Mortimer et al., 2019). In our updated plate kinematic model, the timing of the end of
748 convergence is dependent on two variables: the reconstruction of Osbourn Trough spreading
749 and the choice of Indo-Atlantic mantle reference frame for East Gondwana. We only use the
750 Pacific mantle reference frame of Torsvik et al. (2019), because they showed that previous
751 implementations of Pacific reference frames are flawed. Furthermore, the correctly
752 implemented Pacific hotspot reference frame of Wessel and Kroenke (2008) only leads to more
753 convergence across the Gondwana margin than the model of Torsvik et al. (2019). In all Indo-
754 Atlantic mantle reference frames, convergence continues until the cessation of Osbourn Trough
755 spreading; that is, until 79 Ma in our reconstruction following Mortimer et al. (2019). This
756 reconstruction of the Osbourn Trough leads to c. 1500-2000 km of convergence between the
757 Hikurangi Plate and the Gondwana margin between 100 and 79 Ma, depending on the reference
758 frame (Fig. 9). If future radiometric dating of dredge samples would suggest an older age for the
759 end of Osbourn Trough spreading, the convergence between the Hikurangi Plate and the East
760 Gondwana margin would simply be accommodated by higher rates of spreading and subduction
761 between 120 Ma and any new and reliable date suggested. Even if Osbourn Trough spreading
762 had already ceased by 101 Ma, as interpreted by Zhang and Li (2016), there would still have
763 been 800-1100 km of post-100 Ma convergence between the Pacific Plate and the Zealandia
764 margin (Fig. 9). In this scenario, convergence at the Zealandia margin continued until c. 90 Ma,
765 applying the reference frames of Torsvik et al. (2008) or Doubrovine et al. (2012), or continued
766 until c. 84 Ma (when the Campbell plateau became incorporated in the Pacific Plate) in applying
767 the slab frame of Van der Meer et al. (2010) or the hotspot reference frame of O'Neill et al.
768 (2005).

769 The Hikurangi-Pacific ridge formed a triple junction with the subduction zone located
770 along the margin of East Gondwana, in the vicinity of the Norfolk Ridge (Fig. 6 and 7). North of
771 this Hikurangi-Pacific-Gondwana triple junction, the rate and amount of convergence at the East

772 Gondwana margin were not influenced by spreading at the Osbourn Trough, as the Pacific Plate
773 directly subducted below the Norfolk Ridge. The precise location of this triple junction, where
774 the Pacific-Hikurangi ridge subducted below eastern Gondwana, is uncertain, as it has
775 subsequently been consumed at the Cenozoic Tonga-Kermadec and New Caledonia trenches. In
776 our reconstruction, after 95 Ma we place this triple junction just south of New Caledonia (Fig. 6
777 and 7), which results from the assumption of symmetric spreading between the Pacific and
778 Hikurangi plates between 120 and 79 Ma (see section 4.2.2). The relative motion between the
779 Pacific Plate and the Norfolk Ridge north of the Pacific-Hikurangi-Gondwana triple junction is
780 convergent in all reference frames until at least 90 Ma. In the hotspot reference frames of O'Neill
781 et al. (2005), Torsvik et al. (2008), and Doubrovine et al. (2012), convergence north of the
782 Hikurangi-Pacific-Gondwana triple junction ends at 90 Ma (Fig. 9). In the slab-fitted mantle
783 reference frame of Van der Meer et al. (2010), convergence between the Pacific Plate and the
784 Norfolk Ridge continues until 85 Ma. Subduction south of the New Caledonia sector of the East
785 Gondwana margin thus continued until 90-85 Ma (Fig. 9).

786 In an attempt to reconcile geological (on-land) interpretations of cessation of
787 subduction in New Zealand with oceanic plate reconstructions, Mortimer et al. (2019) proposed
788 a solution to avoid convergence beyond 100 Ma at the Zealandia margin. In this scenario, the
789 Hikurangi Plateau arrives in the trench at 100 Ma, and the Manihiki and Ontong Java plateaus
790 move northwards relative to the margin between 100 and 79 Ma. However, this model places
791 the Pacific plate mosaic ~2250 km farther to the South at 100 Ma than suggested by the hotspot
792 frame of Torsvik et al. (2019) (Fig. 10), which is well beyond the 3° uncertainty assigned to the
793 hotspot model. The solution of Mortimer et al. (2019) therefore does not work in our kinematic
794 reconstruction that combines relative and absolute plate motions; it would require an absolute
795 hotspot wander between 100 and 90-85 Ma of 10-20 cm/yr, for all hotspots below the Pacific
796 Plate, for which there is no evidence, and which is two orders of magnitude faster than typical
797 hotspot motions (e.g., Doubrovine et al., 2012). In addition, we tested whether the latest and
798 highest-detail published isochron sets from the South Pacific realm change the age for the end of
799 convergence across the Gondwana margin that followed from widely used global plate models
800 (e.g., Seton et al., 2012; Müller et al., 2019). And while our updated model differs in detail, for
801 instance in the reconstruction of plates and plate motions in lithosphere that was lost to
802 subduction, the conclusions from those global models are robust: Plate kinematic models leave
803 no room for a cessation of subduction along the Zealandia margin at 100 Ma or before; instead,
804 convergence between the Phoenix Plate's daughters and the East Gondwana margin must have
805 continued until at least 90-85 Ma. Below the New Zealand margin, convergence likely continued
806 even longer if spreading in the Osbourn Trough continued beyond 85 Ma (e.g., 79 Ma according
807 to Mortimer et al., 2019).

808

809

5.2 Reconciling ongoing convergence after 100 Ma with the geology of

810

Zealandia

811

812

813

814

815

816

817

818

Our plate kinematic reconstruction requires that convergence, and by inference subduction, continued until at least 90 Ma along the entire East Gondwana margin, and possibly until 79 Ma below New Zealand and Chatham Rise. While our reconstruction is easily reconciled with the geology of New Caledonia, where subduction-related accretion and magmatism continued until c. 90 Ma (Cluzel et al., 2010; Maurizot et al., 2020b), it conflicts with the common interpretation based on geological observations from New Zealand that subduction there ceased at 105-100 Ma. The observations from New Zealand thus require an alternative explanation.

819

820

821

822

823

824

825

826

827

828

829

830

831

832

833

834

The first often-cited argument for subduction cessation at 105-100 Ma is the timing of the onset of extension that is recognized in the geology of New Zealand (Bradshaw, 1989; Tulloch and Kimbrough, 1989; Field and Uruski, 1997; Laird and Bradshaw, 2004; Crampton et al., 2019), for example in the Canterbury Basin (Barrier et al., 2020). However, extension in the upper plate above an active subduction zone is common, as evidenced by many intra- and back-arc basins across the world. In fact, extension is presently occurring within the Taupo Volcanic Zone in North Island New Zealand, above the Hikurangi subduction zone (e.g., Villamor and Berryman, 2001). In addition, neither numerical models (e.g., Van Hunen and Allen, 2011; Duretz et al., 2014) nor geological observations (Wortel and Spakman, 2000; Webb et al., 2017; Qayyum et al., 2022) suggest a systematic relationship between slab break-off and upper plate extension. It is even questionable whether the onset of extension in East Gondwana, which is recorded from the West Antarctic Rift System to the Tasman Sea region (Gaina et al., 1998; Behrendt, 1999; Fitzgerald, 2002; Raza et al., 2009; Cluzel et al., 2012; Spiegel et al., 2016; Jordan et al., 2020), is directly governed by subduction termination, or related to the intra-continental forces that governed Gondwana breakup. In any case, extension in the Gondwana margin does not necessitate slab break-off and does not exclude ongoing subduction.

835

836

837

838

839

840

841

842

843

The geological interpretation of the cessation of subduction around 105 – 100 Ma is further inferred from interpretation of the geodynamic setting that caused a change in geochemical signature of magmatism in New Zealand. Although the youngest age of ‘normal’ subduction-related I-type magmatism in New Zealand was dated as 128 Ma (Tulloch and Kimbrough, 2003), the 131-105 Ma adakitic magmatism is also considered to be related to ongoing subduction (Tulloch et al., 2009). The subsequent onset of A-type magmatism around 100 Ma is widely regarded as signaling the end of subduction (Tulloch et al., 2009). However, the increase in A-type magmatism is interpreted as the result of thinning of the continental crust of Zealandia during extension, which caused less crustal contamination of the igneous

844 rocks (Tulloch et al., 2009), indicating that these interpretations were made under the
845 assumption that subduction ended around 100 Ma, and no alternative causes were explored.

846 While A-type magmatism is generally interpreted as occurring in the absence of
847 subduction (Loiselle and Wones, 1979), such magmas have also been found in active margin
848 settings, for example related to the arrival of a spreading ridge and the influx of sub-slab mantle
849 to the former wedge (e.g. Zhao et al., 2008; Karsli et al., 2012; Li et al., 2012). We here suggest
850 that the transition to A-type magmatism in New Zealand may also be explained by arrival of a
851 spreading ridge. As explained in section 4.2.3, the plate boundary between the Hikurangi and
852 Aluk plates was likely a spreading ridge south of the Hikurangi Plateau. Our reconstruction
853 predicts that this spreading ridge subducted around 100 Ma below New Zealand (Fig. 7 and 11).
854 The progressive arrival of successively younger oceanic crust before arrival of the spreading
855 ridge may then explain the 128-105 Ma adakitic magmatism, which is often related to the
856 subduction of young oceanic crust (Tulloch and Rabone, 1993).

857 In summary, geological and geochemical interpretations made for New Zealand do not
858 require that subduction ended during c. 105-100 Ma (Fig. 7 and 11). Alternative structural and
859 stratigraphic arguments for the forearc region of New Zealand (Mazengarb and Harris, 1994;
860 Kamp, 1999, 2000; Gardiner and Hall, 2021) are straightforwardly reconciled with ongoing
861 subduction, along with geochemical arguments for the composition of magmatic rocks, which do
862 not exclude ongoing subduction.

863

864 **5.3 Causes for the end of subduction**

865 Why subduction stopped at the margin of East Gondwana in the Cretaceous is puzzling.
866 Explanations for this cessation have so far mostly focused on regional geological features, such
867 as the arrival of a mid-ocean ridge in the trench (Luyendyk, 1995; Bradshaw, 1989; Matthews et
868 al., 2012). The arrival of a mid-ocean ridge in a subduction zone may indeed change the nature
869 of a plate boundary and trigger slab break-off. The nature of the plate boundary that follows
870 upon ridge arrival commonly depends on the relative motion between the original overriding
871 plate and the plate that was formerly spreading with the original down-going plate. For
872 example, west of the active trench below the Antarctic Peninsula, marine magnetic anomalies
873 young from the ocean towards West Antarctica. This shows that subduction below the Antarctic
874 Peninsula indeed ceased due to the arrival of the Aluk-West Antarctica ridge at the trench below
875 West Antarctica, after which relative motion ceased (Eagles, 2004). However, the Hikurangi-
876 Pacific ridge did not subduct parallel to the trench but subducted at an angle to it (Fig. 6C-E and
877 7A-D). Moreover, until the ~84 Ma change in absolute plate motion of the Pacific Plate, the
878 whole Panthalassa mosaic was converging with the East Gondwana margin, which means that
879 subduction continued after the arrival of the Hikurangi-Aluk spreading ridge. More importantly,

880 the newly formed Pacific-Antarctic Ridge did not replace the former subduction zone but cut
881 through the suture and formed at a completely different location (Fig. 6D-E and 7C-D). Ridge
882 arrival is thus not a likely candidate to explain the end of subduction.

883 A second hypothesis for the end of subduction below the Zealandia margin of East
884 Gondwana is the arrival of the Hikurangi Plateau in the trench (e.g., Billen and Stock, 2000; Davy
885 et al., 2008, Davy, 2014; Timm et al., 2014; Reyners et al., 2017; Mortimer et al., 2019). In this
886 hypothesis, the plateau choked the subduction zone after about 150 km of subduction
887 (Riefstahl et al., 2020). However, the Hikurangi Plateau only represents a small portion of the
888 Pacific Plate and only a short length of the trench. If a transform fault could be demonstrated to
889 have bounded the western side of the Hikurangi Plateau, subduction could have continued
890 below the North Island and New Caledonia sections. Moreover, while plateau arrivals at intra-
891 oceanic trenches may cause a polarity reversal (and ongoing subduction), e.g., during the arrival
892 of the Ontong Java Plateau at the Vitiaz trench triggering the formation of the New Hebrides
893 trench and the South Solomon trench (Auzende et al., 1995; Petterson et al., 1997; Quarles van
894 Ufford and Cloos, 2005; Knesel et al., 2008; Lallemand and Arcay, 2021), there is no record of
895 LIP arrival at a trench causing subduction cessation or a plate reorganization on the scale as
896 observed here. Instead, LIP subduction is physically straightforward, even though it may cause
897 shallow dipping slabs (e.g., Yang et al., 2020; Liu et al., 2021). LIP subduction has, for example,
898 been ongoing in the Maracaïbo trench of the southern Caribbean region for more than 50 Ma
899 (White et al., 1999; Boschman et al., 2014), and even the Hikurangi Plateau itself is subducting
900 today at the Hikurangi trench (Collot et al., 1998; Reyners et al., 2011, 2017; Fig. 1), which
901 initiated in the Oligocene (Furlong and Kamp, 2009; Van de Lagemaat et al., 2022). Therefore,
902 while the preservation of the Hikurangi Plateau at the Gondwana margin may suggest that it
903 played a role in determining where the slab broke, it is an unlikely trigger for the cessation of
904 subduction along the entire East Gondwana margin.

905 Instead, we consider it most likely that the end of subduction in the Zealandia sector of
906 East Gondwana was governed by a change in relative plate motion between the Pacific Plate and
907 East Gondwana (Rey and Müller, 2010). More analysis of the driving forces of the Pacific Plate
908 and the Pacific plate mosaic as a whole, not only of local features on the southernmost Pacific
909 Plate could usefully be undertaken. In the East Asia region, below South China, we note that
910 subduction along the continental margin suddenly stopped at around 90-80 Ma (e.g., Cui et al.,
911 2021). Also, in the North Pacific realm there were prominent changes in plate boundary
912 configuration around 90-85 Ma, including the formation of the Kula Plate (Engebretson et al.,
913 1985; Wright et al., 2016), and initiation of intra-oceanic subduction below the Olyutorsky and
914 Kronotsky arcs (Konstantinovskaya, 2002; Shapiro and Solov'ev, 2009; Domeier et al., 2017;
915 Vaes et al., 2019). An analysis of the causes of plate motion change that formed the prelude to

916 the end of subduction below eastern Gondwana requires a detailed kinematic restoration of the
917 plate boundary reorganization, particularly in the enigmatic transition between the Panthalassa
918 and Tethyan domains of SE Asia, which is beyond the scope of this paper.

919

920 **5 Conclusions**

921 We have developed a kinematic reconstruction of the South Pacific and East Gondwana realms
922 back to the Late Jurassic (150 Ma). Our aim was to reconstruct the evolution and destruction of
923 the Phoenix Plate, and to reconcile the geological record of New Zealand with the end of
924 Mesozoic subduction along the East Gondwana margin. From our reconstruction we conclude
925 the following:

- 926 1) Resulting from the emplacement of Ontong Java Nui around 125-120 Ma, the Phoenix
927 Plate broke into at least four plates: The Manihiki, Hikurangi, Chasca, and Aluk plates.
928 During the Late Cretaceous, the Manihiki and Hikurangi plates were captured by the
929 Pacific Plate, while Chasca was captured by the Farallon Plate. Only the Aluk Plate
930 remained an independent tectonic plate into the Cenozoic.
- 931 2) Convergence occurred along the Gondwana margin until 90 or 85 Ma, depending on
932 choice of mantle reference frame. This convergence occurred independent from
933 spreading at the Osbourn Trough and required the presence of a subduction zone along
934 the entire Zealandia margin until at least 90 Ma and possibly until 85 Ma.
- 935 3) Subduction in the New Caledonia region ceased at c. 90 to 85 Ma, but convergence of the
936 Hikurangi Plate with the Chatham Rise must have continued until the cessation of
937 spreading at the Osbourn Trough, recently tentatively estimated at 79 Ma.
- 938 4) The cessation of subduction of the Hikurangi Plate along the entire East Gondwana
939 margin was probably a result of a change in Pacific-Gondwana relative plate motion.
940 This was not due to the arrival of the small Hikurangi Plateau compared with the East
941 Gondwana subduction system.
- 942 5) The 105-100 Ma structural changes within the crust of the overriding New Zealand
943 continental plate may have resulted from subduction of the Aluk-Hikurangi ridge, rather
944 than from the cessation of subduction at the East Gondwana margin.
- 945 6) Geological expressions in the overriding plate may be misleading when used to interpret
946 subduction zone dynamics. While a geological record in the overriding plate may
947 provide evidence for the presence of subduction, absence of such evidence should not be
948 interpreted as conclusive evidence for the absence of subduction.

949

950 **Acknowledgements**

951 DJJvH and SHAvdL acknowledge NWO Vici grant 865.17.001. PJJk acknowledges funding from
952 the New Zealand Government (MBIE Contract: CONT-42907-EMTR-UOW).

953

954 **References**

955 Adams, C. J., Campbell, H. J., Graham, I. J., & Mortimer, N. (1998). Torlesse, Waipapa and Caples
956 suspect terranes of New Zealand: integrated studies of their geological history in relation
957 to neighbouring terranes. *Episodes*, *21*, 235-240.

958 Adams, C. J., Campbell, H. J., & Griffin, W. L. (2007). Provenance comparisons of Permian to
959 Jurassic tectonostratigraphic terranes in New Zealand: perspectives from detrital zircon
960 age patterns. *Geological Magazine*, *144*(4), 701-729.

961 Adams, C. J., Mortimer, N., Campbell, H. J., & Griffin, W. L. (2013). The mid-Cretaceous transition
962 from basement to cover within sedimentary rocks in eastern New Zealand: evidence from
963 detrital zircon age patterns. *Geological Magazine*, *150*(3), 455-478.

964 Amante, C. and Eakins, B.W. (2009). ETOPO1 1 Arc-Minute Global Relief Model: Procedures,
965 Data Sources and Analysis. NOAA Technical Memorandum NESDIS NGDC-24. National
966 Geophysical Data Center, NOAA. doi:10.7289/V5C8276M

967 An, M., Wiens, D. A., Zhao, Y., Feng, M., Nyblade, A. A., Kanao, M., Li, Y., Maggi, A., & L  v  que, J. J.
968 (2015). S-velocity model and inferred Moho topography beneath the Antarctic Plate from
969 Rayleigh waves. *Journal of Geophysical Research: Solid Earth*, *120*(1), 359-383.

970 Atwater, T., & Severinghaus, J. (1989). Tectonic maps of the northeast Pacific. In *The Eastern*
971 *Pacific Ocean and Hawaii*, E. L. Winterer, Donald M. Hussong, Robert W. Decker (Eds).
972 Geological Society of America. <https://doi.org/10.1130/DNAG-GNA-N.15>

973 Auzende, J. M., Pelletier, B., & Eissen, J. P. (1995). The North Fiji Basin geology, structure, and
974 geodynamic evolution. In *Backarc Basins* (pp. 139-175). Springer, Boston, MA.

975 Barckhausen, U., Ranero, C. R., von Huene, R., Cande, S. C., & Roeser, H. A. (2001). Revised
976 tectonic boundaries in the Cocos Plate off Costa Rica: Implications for the segmentation of
977 the convergent margin and for plate tectonic models. *Journal of Geophysical Research:*
978 *Solid Earth*, *106*(B9), 19207-19220.

979 Barckhausen, U., Ranero, C. R., Cande, S. C., Engels, M., & Weinrebe, W. (2008). Birth of an
980 intraoceanic spreading center. *Geology*, *36*(10), 767-770.

981 Barker, P. F. (1982). The Cenozoic subduction history of the Pacific margin of the Antarctic
982 Peninsula: ridge crest–trench interactions. *Journal of the Geological Society*, *139*(6), 787-
983 801.

984 Barrier, A., Nicol, A., Browne, G. H., & Bassett, K. N. (2020). Late Cretaceous coeval multi-
985 directional extension in South Zealandia: Implications for eastern Gondwana
986 breakup. *Marine and Petroleum Geology*, *118*, 104383.

- 987 Behrendt, J. C. (1999). Crustal and lithospheric structure of the West Antarctic Rift System from
988 geophysical investigations—a review. *Global and Planetary Change*, 23(1-4), 25-44.
- 989 Benyshek, Elizabeth K., Paul Wessel, and Brian Taylor. "Tectonic Reconstruction of the Ellice
990 Basin." *Tectonics* 38.11 (2019): 3854-3865.
- 991 Billen, M. I., & Stock, J. (2000). Morphology and origin of the Osbourn Trough. *Journal of*
992 *Geophysical Research: Solid Earth*, 105(B6), 13481-13489.
- 993 Bird, P. (2003). An updated digital model of plate boundaries. *Geochemistry, Geophysics,*
994 *Geosystems*, 4(3).
- 995 Boschman, L. M., van Hinsbergen, D. J., Torsvik, T. H., Spakman, W., & Pindell, J. L. (2014).
996 Kinematic reconstruction of the Caribbean region since the Early Jurassic. *Earth-Science*
997 *Reviews*, 138, 102-136.
- 998 Boschman, L. M., & Van Hinsbergen, D. J. J. (2016). On the enigmatic birth of the Pacific Plate
999 within the Panthalassa Ocean. *Science Advances*, 2(7), e1600022.
- 1000 Boschman, L. M., Van Hinsbergen, D. J. J., Langereis, C. G., Flores, K. E., Kamp, P. J. J., Kimbrough,
1001 D. L., Ueda, H., Van de Lagemaat, S. H. A., Van der Wiel, E. & Spakman, W. (2021a).
1002 Reconstructing lost plates of the panthalassa ocean through Paleomagnetic data from
1003 circum-pacific accretionary orogens. *American Journal of Science*, 321(6), 907-954.
- 1004 Boschman, L. M., van Hinsbergen, D. J., & Spakman, W. (2021b). Reconstructing Jurassic-
1005 Cretaceous Intra-Oceanic Subduction Evolution in the Northwestern Panthalassa Ocean
1006 Using Ocean Plate Stratigraphy From Hokkaido, Japan. *Tectonics*, 40(8), e2019TC005673.
- 1007 Boyden, J. A., Müller, R. D., Gurnis, M., Torsvik, T. H., Clark, J. A., Turner, M., Ivey-Law, H., Watson,
1008 R. J., & Cannon, J. S. (2011). Next-generation plate-tectonic reconstructions using GPlates.
- 1009 Bradshaw, J. D. (1989). Cretaceous geotectonic patterns in the New Zealand
1010 region. *Tectonics*, 8(4), 803-820. <https://doi.org/10.1029/TC008i004p00803>
- 1011 Burton-Johnson, A., & Riley, T. R. (2015). Autochthonous v. accreted terrane development of
1012 continental margins: a revised in situ tectonic history of the Antarctic Peninsula. *Journal of*
1013 *the Geological Society*, 172(6), 822-835.
- 1014 Campbell, M. J., Rosenbaum, G., Allen, C. M., & Mortimer, N. (2020). Origin of dispersed Permian–
1015 Triassic fore-arc basin terranes in New Zealand: Insights from zircon
1016 petrochronology. *Gondwana Research*, 78, 210-227.
- 1017 Cande, S. C., Herron, E. M., & Hall, B. R. (1982). The early Cenozoic tectonic history of the
1018 southeast Pacific. *Earth and Planetary Science Letters*, 57(1), 63-74.
- 1019 Cande, S. C., Raymond, C. A., Stock, J., & Haxby, W. F. (1995). Geophysics of the Pitman Fracture
1020 Zone and Pacific-Antarctic plate motions during the Cenozoic. *Science*, 270(5238), 947-
1021 953.

- 1022 Cande, S. C., & Stock, J. M. (2004a). Pacific—Antarctic—Australia motion and the formation of
1023 the Macquarie Plate. *Geophysical Journal International*, *157*(1), 399-414.
- 1024 Cande, S. C., & Stock, J. M. (2004b). Cenozoic reconstructions of the Australia-new Zealand-south
1025 Pacific sector of antarctica.
- 1026 Cande, S. C., Patriat, P., & Dymant, J. (2010). Motion between the Indian, Antarctic and African
1027 plates in the early Cenozoic. *Geophysical Journal International*, *183*(1), 127-149.
- 1028 Chandler, M. T., Wessel, P., Taylor, B., Seton, M., Kim, S. S., & Hyeong, K. (2012). Reconstructing
1029 Ontong Java Nui: Implications for Pacific absolute plate motion, hotspot drift and true
1030 polar wander. *Earth and Planetary Science Letters*, *331*, 140-151.
- 1031 Cluzel, D., & Meffre, S. (2002). The Boghen terrane (New Caledonia, SW Pacific): a Jurassic
1032 accretionary complex. Preliminary U-Pb radiochronological data on detrital
1033 zircon. *Comptes Rendus Geoscience*, *334*(11), 867-874.
- 1034 Cluzel, D., Adams, C. J., Meffre, S., Campbell, H., & Maurizot, P. (2010). Discovery of Early
1035 Cretaceous rocks in New Caledonia: New geochemical and U-Pb zircon age constraints on
1036 the transition from subduction to marginal breakup in the Southwest Pacific. *The Journal
1037 of Geology*, *118*(4), 381-397.
- 1038 Cluzel, D., Maurizot, P., Collot, J., & Sevin, B. (2012). An outline of the geology of New Caledonia;
1039 from Permian-Mesozoic Southeast Gondwanaland active margin to Cenozoic obduction
1040 and supergene evolution. *Episodes*, *35*(1), 72-86.
- 1041 Choi, H., Kim, S. S., Dymant, J., Granot, R., Park, S. H., & Hong, J. K. (2017). The kinematic
1042 evolution of the Macquarie Plate: A case study for the fragmentation of oceanic
1043 lithosphere. *Earth and Planetary Science Letters*, *478*, 132-142.
- 1044 Collot, J. Y., Lamarche, G., Wood, R. A., Delteil, J., Sosson, M., Lebrun, J. F., & Coffin, M. F. (1995).
1045 Morphostructure of an incipient subduction zone along a transform plate boundary:
1046 Puysegur Ridge and Trench. *Geology*, *23*(6), 519-522.
- 1047 Collot, J. Y., & Davy, B. (1998). Forearc structures and tectonic regimes at the oblique subduction
1048 zone between the Hikurangi Plateau and the southern Kermadec margin. *Journal of
1049 Geophysical Research: Solid Earth*, *103*(B1), 623-650.
- 1050 Cox, A., & Hart, R. B. (1986). Plate Tectonics: How It Works: Blackwell Scientific
1051 Publications. Inc. Boston. 392 pp.
- 1052 Crampton, J. S., Mortimer, N., Bland, K. J., Strogen, D. P., Sagar, M., Hines, B. R., King, P. R., &
1053 Seebeck, H. (2019). Cretaceous termination of subduction at the Zealandia margin of
1054 Gondwana: The view from the paleo-trench. *Gondwana Research*, *70*, 222-242.
1055 <https://doi.org/10.1016/j.gr.2019.01.010>
- 1056 Crameri, F. (2018), Scientific colour maps. Zenodo. <http://doi.org/10.5281/zenodo.1243862>

- 1057 Cramer, F., G.E. Shephard, and P.J. Heron (2020), The misuse of colour in science
1058 communication, *Nature Communications*, 11, 5444. doi: 10.1038/s41467-020-19160-7
- 1059 Croon, M. B., Cande, S. C., & Stock, J. M. (2008). Revised Pacific-Antarctic plate motions and
1060 geophysics of the Menard Fracture Zone. *Geochemistry, Geophysics, Geosystems*, 9(7).
- 1061 Cui, Y., Shao, L., Li, Z. X., Zhu, W., Qiao, P., & Zhang, X. (2021). A Mesozoic Andean-type active
1062 continental margin along coastal South China: New geological records from the basement
1063 of the northern South China Sea. *Gondwana Research*, 99, 36-52.
- 1064 Davy, B., Hoernle, K., & Werner, R. (2008). Hikurangi Plateau: Crustal structure, rifted formation,
1065 and Gondwana subduction history. *Geochemistry, Geophysics, Geosystems*, 9(7).
1066 <https://doi.org/10.1029/2007GC001855>
- 1067 Davy, B. (2014). Rotation and offset of the Gondwana convergent margin in the New Zealand
1068 region following Cretaceous jamming of Hikurangi Plateau large igneous province
1069 subduction. *Tectonics*, 33(8), 1577-1595. <https://doi.org/10.1002/2014TC003629>
- 1070 DeMets, C., & Merkouriev, S. (2019). High-resolution reconstructions of South America plate
1071 motion relative to Africa, Antarctica and North America: 34 Ma to present. *Geophysical
1072 Journal International*, 217(3), 1821-1853.
- 1073 Domeier, M., Shephard, G. E., Jakob, J., Gaina, C., Doubrovine, P. V., & Torsvik, T. H. (2017).
1074 Intraoceanic subduction spanned the Pacific in the Late Cretaceous–Paleocene. *Science
1075 Advances*, 3(11), eaao2303.
- 1076 Doubrovine, P. V., Steinberger, B., & Torsvik, T. H. (2012). Absolute plate motions in a reference
1077 frame defined by moving hot spots in the Pacific, Atlantic, and Indian oceans. *Journal of
1078 Geophysical Research: Solid Earth*, 117(B9).
- 1079 Downey, N. J., Stock, J. M., Clayton, R. W., & Cande, S. C. (2007). History of the Cretaceous
1080 Osborn spreading center. *Journal of Geophysical Research: Solid Earth*, 112(B4).
- 1081 Duretz, T., Gerya, T.V. and Spakman, W., 2014. Slab detachment in laterally varying subduction
1082 zones: 3-D numerical modeling. *Geophysical Research Letters*, 41(6): 1951-1956.
- 1083 Eagles, G. (2004). Tectonic evolution of the Antarctic–Phoenix plate system since 15 Ma. *Earth
1084 and Planetary Science Letters*, 217(1-2), 97-109.
- 1085 Eagles, G., Gohl, K., & Larter, R. D. (2004a). High-resolution animated tectonic reconstruction of
1086 the South Pacific and West Antarctic Margin. *Geochemistry, Geophysics, Geosystems*, 5(7).
- 1087 Eagles, G., Gohl, K., & Larter, R. D. (2004b). Life of the Bellingshausen plate. *Geophysical Research
1088 Letters*, 31(7).
- 1089 Eagles, G., & Scott, B. G. (2014). Plate convergence west of Patagonia and the Antarctic Peninsula
1090 since 61 Ma. *Global and Planetary Change*, 123, 189-198.
- 1091 Eakins, B. W., & Lonsdale, P. F. (2003). Structural patterns and tectonic history of the Bauer
1092 microplate, Eastern Tropical Pacific. *Marine Geophysical Researches*, 24(3), 171-205.

- 1093 Engebretson, D. C., Cox, A., & Gordon, R. G. (1985). Relative motions between oceanic and
1094 continental plates in the Pacific basin. *GSA Special Papers* 206.
1095 <https://doi.org/10.1130/SPE206>
- 1096 Field, B. D., & Uruski, C. I. (1997). *Cretaceous-Cenozoic geology and petroleum systems of the East*
1097 *Coast region, New Zealand* (Vol. 1). Institute of Geological & Nuclear Sciences.
- 1098 Fitzgerald, P. A. U. L. (2002). Tectonics and landscape evolution of the Antarctic plate since the
1099 breakup of Gondwana, with an emphasis on the West Antarctic Rift System and the
1100 Transantarctic Mountains. *Royal Society of New Zealand Bulletin*, 35, 453-469.
- 1101 Gaina, C., Müller, D. R., Royer, J. Y., Stock, J., Hardebeck, J., & Symonds, P. (1998). The tectonic
1102 history of the Tasman Sea: a puzzle with 13 pieces. *Journal of Geophysical Research: Solid*
1103 *Earth*, 103(B6), 12413-12433.
- 1104 Galindo-Zaldívar, J., Gamboa, L., Maldonado, A., Nakao, S., & Bochu, Y. (2004). Tectonic
1105 development of the Bransfield Basin and its prolongation to the South Scotia Ridge,
1106 northern Antarctic Peninsula. *Marine Geology*, 206(1-4), 267-282.
- 1107 Gibbons, A. D., Barckhausen, U., Van Den Bogaard, P., Hoernle, K., Werner, R., Whittaker, J. M., &
1108 Müller, R. D. (2012). Constraining the Jurassic extent of Greater India: Tectonic evolution
1109 of the West Australian margin. *Geochemistry, Geophysics, Geosystems*, 13(5).
- 1110 Gardiner, N. P., & Hall, M. (2021). Discordant forearc deposition and volcanism preceding late-
1111 Cretaceous subduction shutdown in Marlborough, north-eastern South Island, New
1112 Zealand. *Earth-Science Reviews*, 214, 103530.
- 1113 Gardiner, N. P., Hall, M. W., & Cawood, P. A. (2021). A forearc stratigraphic response to
1114 Cretaceous plateau collision and slab detachment, South Island, New
1115 Zealand. *Tectonics*, 40(10), e2021TC006806.
- 1116 Gardiner, N. P., Hall, M., Frears, B. T., & Lovell, R. W. (2022). A stratigraphic record from syn to
1117 post subduction sedimentation in Marlborough, New Zealand, and implications for
1118 Gondwana breakup. *Marine and Petroleum Geology*, 136, 105472.
- 1119 Grobys, J. W., Gohl, K., & Eagles, G. (2008). Quantitative tectonic reconstructions of Zealandia
1120 based on crustal thickness estimates. *Geochemistry, Geophysics, Geosystems*, 9(1).
- 1121 Granot, R., Cande, S. C., Stock, J. M., & Damaske, D. (2013). Revised Eocene-Oligocene kinematics
1122 for the West Antarctic rift system. *Geophysical Research Letters*, 40(2), 279-284.
- 1123 Granot, R., & Dymant, J. (2018). Late Cenozoic unification of East and West Antarctica. *Nature*
1124 *Communications*, 9(1), 1-10.
- 1125 Gurnis, M., Van Avendonk, H., Gulick, S. P., Stock, J., Sutherland, R., Hightower, E., Shuck, B., Patel,
1126 J., Williams, E., Kardell, D., Herzig, E., Idini, B., Graham, K., Estep, J., & Carrington, L. (2019).
1127 Incipient subduction at the contact with stretched continental crust: The Puysegur
1128 Trench. *Earth and Planetary Science Letters*, 520, 212-219.

- 1129 Hall, R. (2002). Cenozoic geological and plate tectonic evolution of SE Asia and the SW Pacific:
1130 computer-based reconstructions, model and animations. *Journal of Asian Earth*
1131 *Sciences*, 20(4), 353-431.
- 1132 Handschumacher, D. W. (1976). Post-Eocene plate tectonics of the eastern Pacific. *The*
1133 *Geophysics of the Pacific Ocean Basin and its Margin*, 19, 177-202.
- 1134 Herron, E.M. and Tucholke, B.E., 1976. Sea-floor magnetic patterns and basement structure in
1135 the southeastern Pacific. In: C.D. Hollister, C. Craddock et al., Initial Reports of the Deep
1136 Sea Drilling Project, 35. U.S. Govt. Printing Office, Washington, D.C. pp. 263-278.
- 1137 Herzer, R. H., Barker, D. H. N., Roest, W. R., & Mortimer, N. (2011). Oligocene-Miocene spreading
1138 history of the northern South Fiji Basin and implications for the evolution of the New
1139 Zealand plate boundary. *Geochemistry, Geophysics, Geosystems*, 12,
1140 Q02004. <https://doi.org/10.1029/2010GC003291>
- 1141 Hochmuth, K., Gohl, K., & Uenzelmann-Neben, G. (2015). Playing jigsaw with large igneous
1142 provinces—A plate tectonic reconstruction of Ontong Java Nui, West Pacific. *Geochemistry,*
1143 *Geophysics, Geosystems*, 16(11), 3789-3807.
- 1144 Hochmuth, K., & Gohl, K. (2017). Collision of Manihiki Plateau fragments to accretional margins
1145 of northern Andes and Antarctic Peninsula. *Tectonics*, 36(2), 229-240.
- 1146 Hoernle, K., Hauff, F., Van den Bogaard, P., Werner, R., Mortimer, N., Geldmacher, J., Garbe-
1147 Schönberg, D., & Davy, B. (2010). Age and geochemistry of volcanic rocks from the
1148 Hikurangi and Manihiki oceanic Plateaus. *Geochimica et Cosmochimica Acta*, 74(24), 7196-
1149 7219.
- 1150 House, M. A., Gurnis, M., Kamp, P. J., & Sutherland, R. (2002). Uplift in the Fiordland region, New
1151 Zealand: Implications for incipient subduction. *Science*, 297(5589), 2038-2041.
- 1152 Iaffaldano, G., Bodin, T., & Sambridge, M. (2012). Reconstructing plate-motion changes in the
1153 presence of finite-rotations noise. *Nature communications*, 3(1), 1-6.
- 1154 Isozaki, Y., Maruyama, S., & Furuoka, F. (1990). Accreted oceanic materials in
1155 Japan. *Tectonophysics*, 181(1-4), 179-205.
- 1156 Isozaki, Y., Aoki, K., Nakama, T., & Yanai, S. (2010). New insight into a subduction-related
1157 orogen: A reappraisal of the geotectonic framework and evolution of the Japanese
1158 Islands. *Gondwana Research*, 18(1), 82-105.
- 1159 Jordan, T. A., Riley, T. R., & Siddoway, C. S. (2020). The geological history and evolution of West
1160 Antarctica. *Nature Reviews Earth & Environment*, 1(2), 117-133.
- 1161 Kamp, P. J. J. (1999). Tracking crustal processes by FT thermochronology in a forearc high
1162 (Hikurangi margin, New Zealand) involving Cretaceous subduction termination and mid-
1163 Cenozoic subduction initiation. *Tectonophysics*, 307(3-4), 313-343.

- 1164 Kamp, P. J. J. (2000). Thermochronology of the Torlesse accretionary complex, Wellington
1165 region, New Zealand. *Journal of Geophysical Research: Solid Earth*, 105(B8), 19253-19272.
- 1166 Karsli, O., Caran, Ş., Dokuz, A., Çoban, H., Chen, B., & Kandemir, R. (2012). A-type granitoids from
1167 the Eastern Pontides, NE Turkey: Records for generation of hybrid A-type rocks in a
1168 subduction-related environment. *Tectonophysics*, 530, 208-224.
- 1169 Knesel, K. M., Cohen, B. E., Vasconcelos, P. M., & Thiede, D. S. (2008). Rapid change in drift of the
1170 Australian plate records collision with Ontong Java plateau. *Nature*, 454(7205), 754-757.
- 1171 Konstantinovskaia, E. A. (2001). Arc–continent collision and subduction reversal in the Cenozoic
1172 evolution of the Northwest Pacific: an example from Kamchatka (NE
1173 Russia). *Tectonophysics*, 333(1-2), 75-94.
- 1174 Laird, M. G., & Bradshaw, J. D. (2004). The break-up of a long-term relationship: the Cretaceous
1175 separation of New Zealand from Gondwana. *Gondwana Research*, 7(1), 273-286.
1176 [https://doi.org/10.1016/S1342-937X\(05\)70325-7](https://doi.org/10.1016/S1342-937X(05)70325-7)
- 1177 Lallemand, S. and Arcay, D. (2021). Subduction initiation from the earliest stages to self-
1178 sustained subduction: Insights from the analysis of 70 Cenozoic sites. *Earth-Science*
1179 *Reviews*, 221: 103779.
- 1180 Larson, R.L. (1997). Superplumes and ridge interactions between Ontong Java and Manihiki
1181 plateaus and the Nova-Canton trough. *Geology*, 25(9): 779-782.
- 1182 Larson, R. L., & Chase, C. G. (1972). Late Mesozoic evolution of the western Pacific
1183 Ocean. *Geological Society of America Bulletin*, 83(12), 3627-3644.
- 1184 Larson, R. L., Pockalny, R. A., Viso, R. F., Erba, E., Abrams, L. J., Luyendyk, B. P., Stock, J. M., &
1185 Clayton, R. W. (2002). Mid-Cretaceous tectonic evolution of the Tongareva triple junction
1186 in the southwestern Pacific Basin. *Geology*, 30(1), 67-70.
- 1187 Larter, R. D., & Barker, P. F. (1991). Effects of ridge crest-trench interaction on Antarctic-
1188 Phoenix spreading: forces on a young subducting plate. *Journal of Geophysical Research:*
1189 *Solid Earth*, 96(B12), 19583-19607.
- 1190 Larter, R. D., Cunningham, A. P., Barker, P. F., Gohl, K., & Nitsche, F. O. (2002). Tectonic evolution
1191 of the Pacific margin of Antarctica 1. Late Cretaceous tectonic reconstructions. *Journal of*
1192 *Geophysical Research: Solid Earth*, 107(B12), EPM-5.
1193 <https://doi.org/10.1029/2000JB000052>
- 1194 Lawver, L. A., & Gahagan, L. M. (1994). Constraints on timing of extension in the Ross Sea
1195 region. *Terra Antarctica*, 1(3), 545-552.
- 1196 Li, H., Ling, M. X., Li, C. Y., Zhang, H., Ding, X., Yang, X. Y., ... & Sun, W. D. (2012). A-type granite
1197 belts of two chemical subgroups in central eastern China: Indication of ridge
1198 subduction. *Lithos*, 150, 26-36.

- 1199 Llubes, M., Seoane, L., Bruinsma, S., & Rémy, F. (2018). Crustal thickness of Antarctica estimated
1200 using data from gravimetric satellites. *Solid Earth*, 9(2), 457-467.
- 1201 Loiselle, M.C., and Wones, D.R., 1979, Characteristics and origin of anorogenic granites:
1202 Geological Society of America Abstracts with Programs, v. 11, p. 468.
- 1203 Luyendyk, B. P. (1995). Hypothesis for Cretaceous rifting of east Gondwana caused by
1204 subducted slab capture. *Geology*, 23(4), 373-376. [https://doi.org/10.1130/0091-](https://doi.org/10.1130/0091-7613(1995)023<0373:HFCROE>2.3.CO;2)
1205 [7613\(1995\)023<0373:HFCROE>2.3.CO;2](https://doi.org/10.1130/0091-7613(1995)023<0373:HFCROE>2.3.CO;2)
- 1206 Mahoney, J. J., Storey, M., Duncan, R. A., Spencer, K. J., & Pringle, M. (1993). Geochemistry and age
1207 of the Ontong Java Plateau. *The Mesozoic Pacific: Geology, Tectonics, and Volcanism*,
1208 *Geophys. Monogr. Ser.*, 77, 233-261.
- 1209 Matthews, K. J., Müller, R. D., Wessel, P., & Whittaker, J. M. (2011). The tectonic fabric of the
1210 ocean basins. *Journal of Geophysical Research: Solid Earth*, 116(B12).
- 1211 Matthews, K. J., Seton, M., & Müller, R. D. (2012). A global-scale plate reorganization event at
1212 105–100 Ma. *Earth and Planetary Science Letters*, 355, 283-298.
1213 <https://doi.org/10.1016/j.epsl.2012.08.023>
- 1214 Matthews, K. J., Williams, S. E., Whittaker, J. M., Müller, R. D., Seton, M., & Clarke, G. L. (2015).
1215 Geologic and kinematic constraints on Late Cretaceous to mid Eocene plate boundaries in
1216 the southwest Pacific. *Earth-Science Reviews*, 140, 72-107.
- 1217 Maurizot, P., Cluzel, D., Patriat, M., Collot, J., Iseppi, M., Lesimple, S., Sechiari, A., Bosch, D.,
1218 Montanini, A., Macera, P., & Davies, H. L. (2020a). The Eocene subduction–obduction
1219 complex of New Caledonia. *Geological Society, London, Memoirs*, 51(1), 93-130.
- 1220 Maurizot, P., Cluzel, D., Meffre, S., Campbell, H. J., Collot, J., & Sevin, B. (2020b). Pre-Late
1221 Cretaceous basement terranes of the Gondwana active margin of New
1222 Caledonia. *Geological Society, London, Memoirs*, 51(1), 27-52.
- 1223 Mazengarb, C., & Harris, D. H. M. (1994). Cretaceous stratigraphic and structural relations of
1224 Raukumara Peninsula, New Zealand: stratigraphic patterns associated with the migration
1225 of a thrust system. In *Annales Tectonicae* (Vol. 8, pp. 100-118).
- 1226 McCarron, J. J., & Larter, R. D. (1998). Late Cretaceous to early Tertiary subduction history of the
1227 Antarctic Peninsula. *Journal of the Geological Society*, 155(2), 255-268.
- 1228 McCarthy, A., Magri, L., Sauermilch, I., Fox, J., Seton, M., Mohn, G., Tugend, J., Feig, S., Falloon, T., &
1229 Whittaker, J. M. The Louisiade ophiolite: a missing link in the western Pacific. *Terra Nova*.
- 1230 Molnar, P., Atwater, T., Mammerickx, J., & Smith, S. M. (1975). Magnetic anomalies, bathymetry
1231 and the tectonic evolution of the South Pacific since the Late Cretaceous. *Geophysical*
1232 *Journal International*, 40(3), 383-420.
- 1233 Mortimer, N. (2004). New Zealand's geological foundations. *Gondwana research*, 7(1), 261-272.

- 1234 Mortimer, N., Hoernle, K., Hauff, F., Palin, J. M., Dunlap, W. J., Werner, R., & Faure, K. (2006). New
1235 constraints on the age and evolution of the Wishbone Ridge, southwest Pacific Cretaceous
1236 microplates, and Zealandia–West Antarctica breakup. *Geology*, *34*(3), 185-188.
- 1237 Mortimer, N., Rattenbury, M. S., King, P. R., Bland, K. J., Barrell, D. J. A., Bache, F., Begg, J. G.,
1238 Campbell, H. J., Cox, S. C., Crampton, J. S., Edbrooke, S. W., Forsyth, P. J., Johnston, M. R.,
1239 Jongens, R., Lee, J. M., Leonard, G. S., Raine, J. I., Skinner, D. N. B., Timm, C., Townsend, D. B.,
1240 Tulloch, A. J., Turnbull, I. M., & Turnbull, R. E. (2014). High-level stratigraphic scheme for
1241 New Zealand rocks. *New Zealand Journal of Geology and Geophysics*, *57*(4), 402-419.
- 1242 Mortimer, N., Campbell, H. J., Tulloch, A. J., King, P. R., Stagpoole, V. M., Wood, R. A., Rattenbury,
1243 M.S., Sutherland, R., Adams, C. J., Collot, J. & Seton, M. (2017). Zealandia: Earth's hidden
1244 continent. *GSA today*, *27*(3), 27-35.
- 1245 Mortimer, N., van den Bogaard, P., Hoernle, K., Timm, C., Gans, P. B., Werner, R., & Riefstahl, F.
1246 (2019). Late Cretaceous oceanic plate reorganization and the breakup of Zealandia and
1247 Gondwana. *Gondwana Research*, *65*, 31-42. <https://doi.org/10.1016/j.gr.2018.07.010>
- 1248 Mueller, C. O., & Jokat, W. (2019). The initial Gondwana break-up: a synthesis based on new
1249 potential field data of the Africa-Antarctica Corridor. *Tectonophysics*, *750*, 301-328.
- 1250 Müller, R. D., Cannon, J., Qin, X., Watson, R. J., Gurnis, M., Williams, S., Pfaffelmoser, T., Seton, M.,
1251 Russel, S. H. J., & Zahirovic, S. (2018). GPlates: building a virtual Earth through deep
1252 time. *Geochemistry, Geophysics, Geosystems*, *19*(7), 2243-2261.
- 1253 Müller, R. D., Zahirovic, S., Williams, S. E., Cannon, J., Seton, M., Bower, D. J., Tetley, M. G., Heine,
1254 C., Le Breton, E., Liu, S., Russel, S. H. J., Yang, T., Leonard, J., & Gurnis, M. (2019). A global
1255 plate model including lithospheric deformation along major rifts and orogens since the
1256 Triassic. *Tectonics*, *38*(6), 1884-1907. <https://doi.org/10.1029/2018TC005462>
- 1257 Muir, R. J., Ireland, T. R., Weaver, S. D., Bradshaw, J. D., Waight, T. E., Jongens, R., & Eby, G. N.
1258 (1997). SHRIMP U-Pb geochronology of Cretaceous magmatism in northwest Nelson-
1259 Westland, South Island, New Zealand. *New Zealand Journal of Geology and*
1260 *Geophysics*, *40*(4), 453-463. <https://doi.org/10.1080/00288306.1997.9514775>
- 1261 Nakanishi, M., Tamaki, K., & Kobayashi, K. (1992). Magnetic anomaly lineations from Late
1262 Jurassic to Early Cretaceous in the west-central Pacific Ocean. *Geophysical Journal*
1263 *International*, *109*(3), 701-719.
- 1264 Nakanishi, M., & Winterer, E. L. (1998). Tectonic history of the Pacific-Farallon-Phoenix triple
1265 junction from Late Jurassic to Early Cretaceous: an abandoned Mesozoic spreading system
1266 in the central Pacific basin. *Journal of Geophysical Research: Solid Earth*, *103*(B6), 12453-
1267 12468.
- 1268 NOAA National Geophysical Data Center (2009). ETOPO1 1 Arc-Minute Global Relief Model.
1269 NOAA National Centers for Environmental Information.

- 1270 O'Neill, C., Müller, D., & Steinberger, B. (2005). On the uncertainties in hot spot reconstructions
1271 and the significance of moving hot spot reference frames. *Geochemistry, Geophysics,*
1272 *Geosystems*, 6(4).
- 1273 Ogg, J. G. (2020). Geomagnetic polarity time scale
1274 In F.M. Gradstein, J.G. Ogg, M.D. Schmitz, G.M. Ogg (Eds.), *Geologic Time Scale*
1275 *2020*, Elsevier, Amsterdam (2020), pp. 159-192,
- 1276 Pepper, M., Gehrels, G., Pullen, A., Ibanez-Mejia, M., Ward, K. M., & Kapp, P. (2016). Magmatic
1277 history and crustal genesis of western South America: Constraints from U-Pb ages and Hf
1278 isotopes of detrital zircons in modern rivers. *Geosphere*, 12(5), 1532-1555.
- 1279 Petterson, M. G., Neal, C. R., Mahoney, J. J., Kroenke, L. W., Saunders, A. D., Babbs, T. L., Duncan, R.
1280 A., Tolia, D., & McGrail, B. (1997). Structure and deformation of north and central Malaita,
1281 Solomon Islands: tectonic implications for the Ontong Java Plateau-Solomon arc collision,
1282 and for the fate of oceanic plateaus. *Tectonophysics*, 283(1-4), 1-33.
- 1283 Pindell, J.L. and Kennan, L. (2009). Tectonic evolution of the Gulf of Mexico, Caribbean and
1284 northern South America in the mantle reference frame: an update. Geological Society,
1285 London, Special Publications, 328(1): 1.1-55.
- 1286 Qayyum, A., Lom, N., Advokaat, E.L., Spakman, W., van der Meer, D.G. and van Hinsbergen, D.J.J.
1287 (2022). Subduction and slab detachment under moving trenches during ongoing India-
1288 Asia convergence. *Earth and Space Science Open Archive*: 45.
- 1289 Quarles van Ufford, A., & Cloos, M. (2005). Cenozoic tectonics of New Guinea. *AAPG*
1290 *bulletin*, 89(1), 119-140.
- 1291 Raza, A., Hill, K. C., & Korsch, R. J. (2009). Mid-Cretaceous uplift and denudation of the Bowen
1292 and Surat Basins, eastern Australia: relationship to Tasman Sea rifting from apatite
1293 fission-track and vitrinite-reflectance data. *Australian Journal of Earth Sciences*, 56(3),
1294 501-531.
- 1295 Rey, P., Müller, R. (2010) Fragmentation of active continental plate margins owing to the
1296 buoyancy of the mantle wedge. *Nature Geosci* 3, 257–261.
1297 <https://doi.org/10.1038/ngeo825>
- 1298 Reyners, M., Eberhart-Phillips, D., & Bannister, S. (2011). Tracking repeated subduction of the
1299 Hikurangi Plateau beneath New Zealand. *Earth and Planetary Science Letters*, 311(1-2),
1300 165-171.
- 1301 Reyners, M., Eberhart-Phillips, D., Upton, P., & Gubbins, D. (2017). Three-dimensional imaging of
1302 impact of a large igneous province with a subduction zone. *Earth and Planetary Science*
1303 *Letters*, 460, 143-151.
- 1304 Riefstahl, F., Gohl, K., Davy, B., Hoernle, K., Mortimer, N., Timm, C., Werner, R., & Hochmuth, K.
1305 (2020). Cretaceous intracontinental rifting at the southern Chatham Rise margin and

- 1306 initialisation of seafloor spreading between Zealandia and Antarctica. *Tectonophysics*, 776,
1307 228298.
- 1308 Schellart, W. P., Lister, G. S., & Toy, V. G. (2006). A Late Cretaceous and Cenozoic reconstruction
1309 of the Southwest Pacific region: tectonics controlled by subduction and slab rollback
1310 processes. *Earth-Science Reviews*, 76(3-4), 191-233.
- 1311 Sdrolias, M., Müller, R. D., & Gaina, C. (2003). Tectonic evolution of the southwest Pacific using
1312 constraints from backarc basins. *Geological Society of America Special Papers*, 372, 343–
1313 359.
- 1314 Seton, M., Müller, R. D., Zahirovic, S., Gaina, C., Torsvik, T., Shephard, G., Talsma, A., Gurnis, M.,
1315 Maus, S., & Chandler, M. (2012). Global continental and ocean basin reconstructions since
1316 200 Ma. *Earth-Science Reviews*, 113(3-4), 212-270.
1317 <https://doi.org/10.1016/j.earscirev.2012.03.002>
- 1318 Seton, M., Whittaker, J. M., Wessel, P., Müller, R. D., DeMets, C., Merkuriev, S., Cande, S., Eagles,
1319 G., Granot, R., Stock, J., Wright, N., Williams, S. E. (2014). Community infrastructure and
1320 repository for marine magnetic identifications. *Geochemistry, Geophysics,*
1321 *Geosystems*, 15(4), 1629-1641.
- 1322 Shapiro, M. N., & Solov'ev, A. V. (2009). Formation of the Olyutorsky–Kamchatka foldbelt: A
1323 kinematic model. *Russian Geology and Geophysics*, 50(8), 668-681.
- 1324 Shen, W., Wiens, D. A., Anandkrishnan, S., Aster, R. C., Gerstoft, P., Bromirski, P. D., Hansen, S. E.,
1325 Dalziel, I. W. D., Heeszel, D. S., Huerta, A. D., Nyblade, A. A., Stephen, R., Wilson, T. J., &
1326 Winberry, J. P. (2018). The crust and upper mantle structure of central and West
1327 Antarctica from Bayesian inversion of Rayleigh wave and receiver functions. *Journal of*
1328 *Geophysical Research: Solid Earth*, 123(9), 7824-7849.
- 1329 Sliter, W. V., Ishizaki, K., & Saito, T. (1992). Cretaceous planktonic foraminiferal biostratigraphy
1330 and paleoceanographic events in the Pacific Ocean with emphasis on indurated
1331 sediment. *Centenary of Japanese Micropaleontology*, 281-99.
- 1332 Smith, T. R., & Cole, J. W. (1997). Somers ignimbrite formation: Cretaceous high-grade
1333 ignimbrites from South Island, New Zealand. *Journal of Volcanology and Geothermal*
1334 *Research*, 75(1-2), 39-57.
- 1335 Spiegel, C., Lindow, J., Kamp, P. J., Meisel, O., Mukasa, S., Lisker, F., Kuhn, G., & Gohl, K. (2016).
1336 Tectonomorphic evolution of Marie Byrd Land–Implications for Cenozoic rifting activity
1337 and onset of West Antarctic glaciation. *Global and Planetary Change*, 145, 98-115.
- 1338 Steinberger, B., Sutherland, R., & O'Connell, R. J. (2004). Prediction of Emperor-Hawaii seamount
1339 locations from a revised model of global plate motion and mantle flow. *Nature*, 430(6996),
1340 167-173.

- 1341 Stock, J. M., & Cande, S. C. (2002). Tectonic history of Antarctic seafloor in the Australia-New
1342 Zealand-South Pacific sector: Implications for Antarctic continental tectonics.
- 1343 Stock, J., & Molnar, P. (1987). Revised history of early Tertiary plate motion in the south-west
1344 Pacific. *Nature*, 325(6104), 495-499.
- 1345 Sutherland, R., & Hollis, C. (2001). Cretaceous demise of the Moa plate and strike-slip motion at
1346 the Gondwana margin. *Geology*, 29(3), 279-282.
- 1347 Taylor, B. (2006). The single largest oceanic plateau: Ontong Java–Manihiki–Hikurangi. *Earth
1348 and Planetary Science Letters*, 241(3-4), 372-380.
- 1349 Tebbens, S. F., & Cande, S. C. (1997). Southeast Pacific tectonic evolution from early Oligocene to
1350 present. *Journal of Geophysical Research: Solid Earth*, 102(B6), 12061-12084.
- 1351 Tebbens, S. F., Cande, S. C., Kovacs, L., Parra, J. C., LaBrecque, J. L., & Vergara, H. (1997). The Chile
1352 ridge: A tectonic framework. *Journal of Geophysical Research: Solid Earth*, 102(B6), 12035-
1353 12059.
- 1354 Timm, C., Hoernle, K., Werner, R., Hauff, F., van den Bogaard, P., Michael, P., Coffin, M. F., &
1355 Koppers, A. (2011). Age and geochemistry of the oceanic Manihiki Plateau, SW Pacific:
1356 New evidence for a plume origin. *Earth and Planetary Science Letters*, 304(1-2), 135-146.
- 1357 Torsvik, T. H., Müller, R. D., Van der Voo, R., Steinberger, B., & Gaina, C. (2008). Global plate
1358 motion frames: toward a unified model. *Reviews of geophysics*, 46(3).
- 1359 Torsvik, T. H., Steinberger, B., Shephard, G. E., Doubrovine, P. V., Gaina, C., Domeier, M., Conrad,
1360 C. P., & Sager, W. W. (2019). Pacific-Panthalassic reconstructions: Overview, errata and
1361 the way forward. *Geochemistry, Geophysics, Geosystems*, 20(7), 3659-3689.
1362 <https://doi.org/10.1029/2019GC008402>
- 1363 Tulloch, A. J., & Kimbrough, D. L. (1989). The Paparoa metamorphic core complex, New Zealand:
1364 cretaceous extension associated with fragmentation of the Pacific margin of
1365 Gondwana. *Tectonics*, 8(6), 1217-1234.
- 1366 Tulloch, A. J., Kimbrough, D. L., Landis, C. A., Mortimer, N., & Johnston, M. R. (1999).
1367 Relationships between the Brook Street terrane and Median Tectonic Zone (Median
1368 batholith): evidence from Jurassic conglomerates. *New Zealand Journal of Geology and
1369 Geophysics*, 42(2), 279-293.
- 1370 Tulloch, A. J., & Rabone, S. D. C. (1993). Mo-bearing granodiorite porphyry plutons of the Early
1371 Cretaceous Separation Point Suite, west Nelson, New Zealand. *New Zealand journal of
1372 geology and geophysics*, 36(4), 401-408.
- 1373 Tulloch A. J. & Kimbrough D. L. (2003) in *Tectonic Evolution of Northwestern Mexico and the
1374 Southwestern USA*, Paired plutonic belts in convergent margins and the development of
1375 high Sr/Y magmatism: Peninsular Ranges batholith of Baja-California and Median
1376 batholith of New Zealand, Geological Society of America Special Papers, eds Johnson S.

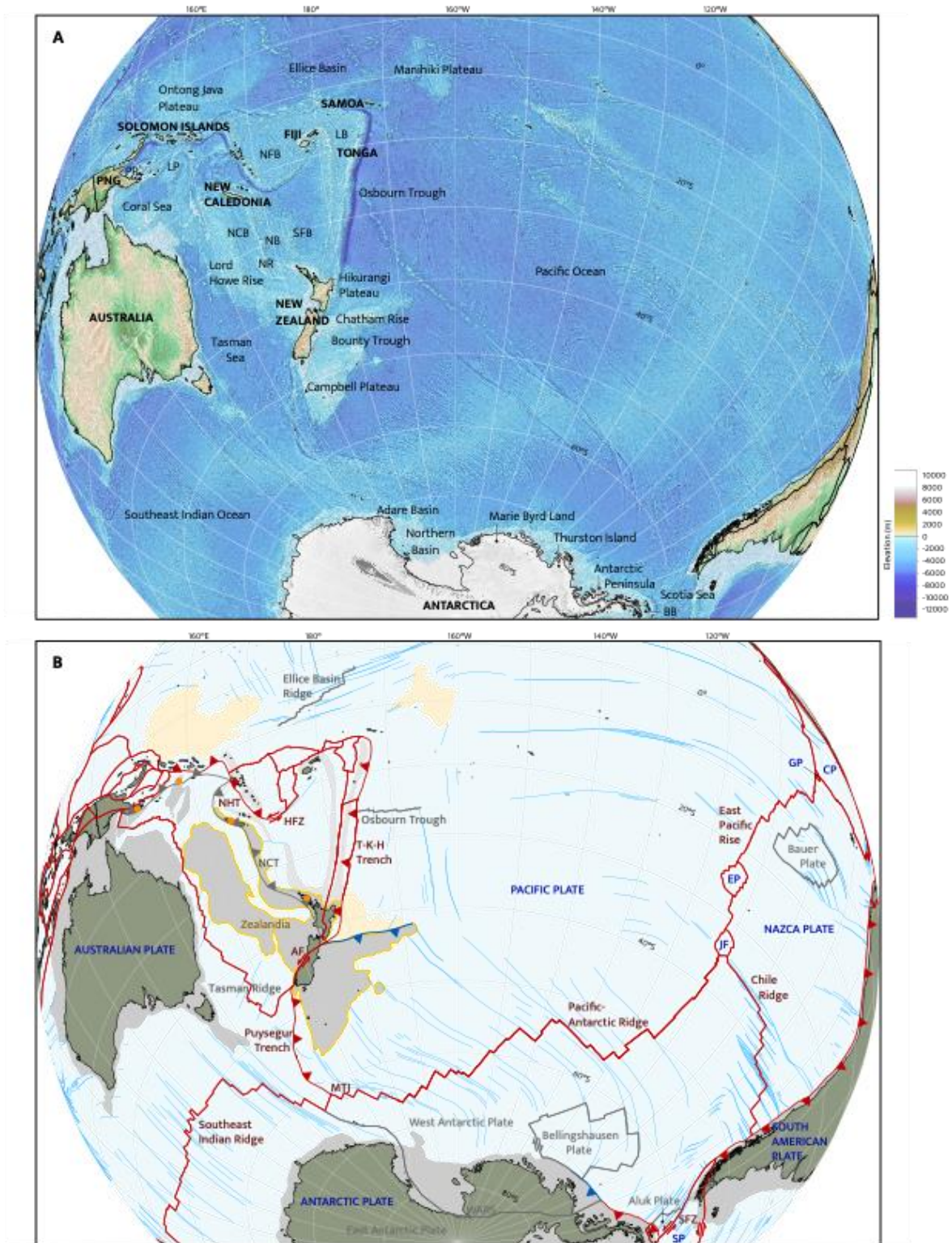
- 1377 E., Paterson S. R., Fletcher J. M., Girty G. H., Kimbrough D. L., Martín-Barajas A. 374,
1378 pp 275–295
- 1379 Tulloch, A. J., Ramezani, J., Mortimer, N., Mortensen, J., van den Bogaard, P., & Maas, R. (2009).
1380 Cretaceous felsic volcanism in New Zealand and Lord Howe Rise (Zealandia) as a
1381 precursor to final Gondwana break-up. *Geological Society, London, Special*
1382 *Publications*, 321(1), 89-118. <https://doi.org/10.1144/SP321.5>
- 1383 Vaes, B., Van Hinsbergen, D. J. J., & Boschman, L. M. (2019). Reconstruction of subduction and
1384 back-arc spreading in the NW Pacific and Aleutian Basin: Clues to causes of Cretaceous
1385 and Eocene plate reorganizations. *Tectonics*, 38(4), 1367-1413.
- 1386 Van de Lagemaat, S. H.A, Van Hinsbergen, D. J. J., Boschman, L. M., Kamp, P. J. J., & Spakman, W.
1387 (2018a). Southwest Pacific absolute plate kinematic reconstruction reveals major
1388 Cenozoic Tonga-Kermadec slab dragging. *Tectonics*, 37(8), 2647-2674.
- 1389 Van de Lagemaat, S. H.A, Boschman, L. M., Kamp, P. J. J., Langereis, C. G., & van Hinsbergen, D. J. J.
1390 (2018b). Post-remagnetisation vertical axis rotation and tilting of the Murihiku Terrane
1391 (North Island, New Zealand). *New Zealand Journal of Geology and Geophysics*, 61(1), 9-25.
- 1392 Van de Lagemaat, S. H. A., Swart, M. L., Vaes, B., Kusters, M. E., Boschman, L. M., Burton-Johnson,
1393 A., Bijl, P. K., Spakman, W., & Van Hinsbergen, D. J. J. (2021). Subduction initiation in the
1394 Scotia Sea region and opening of the Drake Passage: When and why?. *Earth-Science*
1395 *Reviews*, 215, 103551.
- 1396 Van Der Meer, D. G., Spakman, W., Van Hinsbergen, D. J., Amaru, M. L., & Torsvik, T. H. (2010).
1397 Towards absolute plate motions constrained by lower-mantle slab remnants. *Nature*
1398 *Geoscience*, 3(1), 36-40.
- 1399 Van der Meer, Q. H., Storey, M., Scott, J. M., & Waight, T. E. (2016). Abrupt spatial and
1400 geochemical changes in lamprophyre magmatism related to Gondwana fragmentation
1401 prior, during and after opening of the Tasman Sea. *Gondwana Research*, 36, 142-156.
1402 <https://doi.org/10.1016/j.gr.2016.04.004>
- 1403 Van der Meer, Q. H. A., Waight, T. E., Scott, J. M., & Münker, C. (2017). Variable sources for
1404 Cretaceous to recent HIMU and HIMU-like intraplate magmatism in New Zealand. *Earth*
1405 *and Planetary Science Letters*, 469, 27-41. <https://doi.org/10.1016/j.epsl.2017.03.037>
- 1406 Van Der Meer, Q. H. A., Waight, T. E., Tulloch, A. J., Whitehouse, M. J., & Andersen, T. (2018).
1407 Magmatic evolution during the Cretaceous transition from subduction to continental
1408 break-up of the Eastern Gondwana margin (New Zealand) documented by in-situ zircon
1409 O–Hf isotopes and bulk-rock Sr–Nd isotopes. *Journal of Petrology*, 59(5), 849-880.
1410 <https://doi.org/10.1093/petrology/egy047>

- 1411 Van Hinsbergen, D. J., & Schouten, T. L. (2021). Deciphering paleogeography from orogenic
1412 architecture: constructing orogens in a future supercontinent as thought
1413 experiment. *American Journal of Science*, 321(6), 955-1031.
- 1414 Van Hunen, J. and Allen, M.B., 2011. Continental collision and slab break-off: A comparison of 3-
1415 D numerical models with observations. *Earth and Planetary Science Letters*, 302(1-2): 27-
1416 37.
- 1417 Veevers, J. J. (2012). Reconstructions before rifting and drifting reveal the geological
1418 connections between Antarctica and its conjugates in Gondwanaland. *Earth-Science*
1419 *Reviews*, 111(3-4), 249-318.
- 1420 Villamor, P., & Berryman, K. (2001). A late Quaternary extension rate in the Taupo Volcanic
1421 Zone, New Zealand, derived from fault slip data. *New Zealand Journal of Geology and*
1422 *Geophysics*, 44(2), 243-269.
- 1423 Viso, R. F., Larson, R. L., & Pockalny, R. A. (2005). Tectonic evolution of the Pacific–Phoenix–
1424 Farallon triple junction in the South Pacific Ocean. *Earth and Planetary Science*
1425 *Letters*, 233(1-2), 179-194.
- 1426 Waight, T. E., Weaver, S. D., & Muir, R. J. (1998). Mid-Cretaceous granitic magmatism during the
1427 transition from subduction to extension in southern New Zealand: a chemical and tectonic
1428 synthesis. *Lithos*, 45(1-4), 469-482. [https://doi.org/10.1016/S0024-4937\(98\)00045-0](https://doi.org/10.1016/S0024-4937(98)00045-0)
- 1429 Webb, A.A.G., Guo, H., Clift, P.D., Husson, L., Müller, T., Costantino, D., Yin, A., Xu, Z., Cao, H. and
1430 Wang, Q. (2017). The Himalaya in 3D: Slab dynamics controlled mountain building and
1431 monsoon intensification. *Lithosphere*.
- 1432 Wessel, P., Matthews, K. J., Müller, R. D., Mazzoni, A., Whittaker, J. M., Myhill, R., & Chandler, M. T.
1433 (2015). *Semiautomatic fracture zone tracking* (Vol. 16, No. 7, pp. 2462-2472).
- 1434 Whattam, S. A., Malpas, J., Smith, I. E., & Ali, J. R. (2006). Link between SSZ ophiolite formation,
1435 emplacement and arc inception, Northland, New Zealand: U–Pb SHRIMP constraints;
1436 Cenozoic SW Pacific tectonic implications. *Earth and Planetary Science Letters*, 250(3-4),
1437 606-632.
- 1438 Whattam, S. A., Malpas, J., Ali, J. R., & Smith, I. E. (2008). New SW Pacific tectonic model: Cyclical
1439 intraoceanic magmatic arc construction and near-coeval emplacement along the
1440 Australia-Pacific margin in the Cenozoic. *Geochemistry, Geophysics, Geosystems*, 9(3).
- 1441 Whattam, S.A. and Stern, R.J. (2015). Late Cretaceous plume-induced subduction initiation along
1442 the southern margin of the Caribbean and NW South America: The first documented
1443 example with implications for the onset of plate tectonics. *Gondwana Research*, 27(1): 38-
1444 63. Whittaker, J. M., Muller, R. D., Leitchenkov, G., Stagg, H., Sdrolias, M., Gaina, C., &
1445 Goncharov, A. (2007). Major Australian–Antarctic plate reorganization at Hawaiian–
1446 Emperor bend time. *Science*, 318(5847), 83-86.

- 1447 White, R. V., Tarney, J., Kerr, A. C., Saunders, A. D., Kempton, P. D., Pringle, M. S., & Klaver, G. T.
1448 (1999). Modification of an oceanic plateau, Aruba, Dutch Caribbean: implications for the
1449 generation of continental crust. *Lithos*, *46*(1), 43-68.
- 1450 Whittaker, J. M., Williams, S. E., & Müller, R. D. (2013). Revised tectonic evolution of the Eastern
1451 Indian Ocean. *Geochemistry, Geophysics, Geosystems*, *14*(6), 1891-1909.
- 1452 Wilder, Douglas T., "Relative Motion History of the Pacific-Nazca (Farallon) Plates since 30
1453 Million Years Ago" (2003). *USF Tampa Graduate Theses and Dissertations*.
1454 <https://digitalcommons.usf.edu/etd/1506>
- 1455 Williams, S. E., Whittaker, J. M., & Müller, R. D. (2011). Full-fit, palinspastic reconstruction of the
1456 conjugate Australian-Antarctic margins. *Tectonics*, *30*(6).
- 1457 Winterer, E. L., Lonsdale, P. F., Matthews, J. L., & Rosendahl, B. R. (1974, October). Structure and
1458 acoustic stratigraphy of the Manihiki Plateau. In *Deep Sea Research and Oceanographic*
1459 *Abstracts* (Vol. 21, No. 10, pp. 793-813). Elsevier.
- 1460 Wobbe, F., Gohl, K., Chambord, A., & Sutherland, R. (2012). Structure and breakup history of the
1461 rifted margin of West Antarctica in relation to Cretaceous separation from Zealandia and
1462 Bellingshausen plate motion. *Geochemistry, Geophysics, Geosystems*, *13*(4).
1463 <https://doi.org/10.1029/2011GC003742>
- 1464 Wortel, M.J.R. and Spakman, W., 2000. Subduction and slab detachment in the Mediterranean-
1465 Carpathian region. *Science*, *290*(5498): 1910-1917.
- 1466 Worthington, T. J., Hekinian, R., Stoffers, P., Kuhn, T., & Hauff, F. (2006). Osbourn Trough:
1467 Structure, geochemistry and implications of a mid-Cretaceous paleospreading ridge in the
1468 South Pacific. *Earth and Planetary Science Letters*, *245*(3-4), 685-701.
- 1469 Wright, N. M., Seton, M., Williams, S. E., & Mueller, R. D. (2016). The Late Cretaceous to recent
1470 tectonic history of the Pacific Ocean basin. *Earth-Science Reviews*, *154*, 138-173.
1471 <https://doi.org/10.1016/j.earscirev.2015.11.015>
- 1472 Yan, C. Y., & Kroenke, L. W. (1993). A plate tectonic reconstruction of the Southwest Pacific, 0-
1473 100 Ma. *Oceanic Drilling Program, Scientific Results*, **130**, 697-709.
- 1474 Yang, T., Liu, S., Guo, P., Leng, W., & Yang, A. (2020). Yanshanian orogeny during North China's
1475 drifting away from the trench: Implications of numerical models. *Tectonics*, *39*(12),
1476 e2020TC006350.
- 1477 Zhang, G. L., & Li, C. (2016). Interactions of the Greater Ontong Java mantle plume component
1478 with the Osbourn Trough. *Scientific Reports*, *6*(1), 1-8.
- 1479 Zhao, X. F., Zhou, M. F., Li, J. W., & Wu, F. Y. (2008). Association of Neoproterozoic A- and I-type
1480 granites in South China: implications for generation of A-type granites in a subduction-
1481 related environment. *Chemical Geology*, *257*(1-2), 1-15.
- 1482

1484 **Figures**

1485



1486

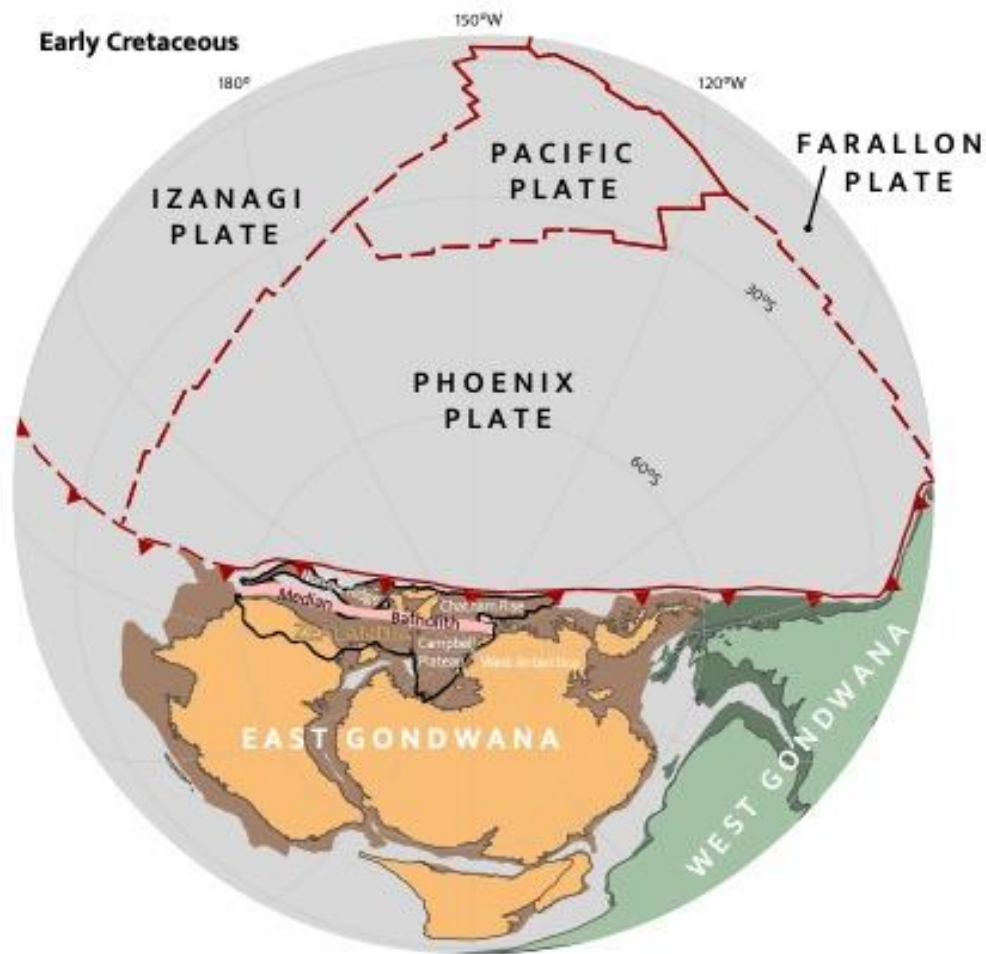
1487 **Fig. 1:** Present-day geographic and tectonic maps of the South Pacific region.

1488 **A) Geographic map**

1489 BB: Bransfield Basin; LB: Lau Basin; LP: Louisiade Plateau; NB: Norfolk Basin; NCB: New
1490 Caledonia Basin; NFB: North Fiji Basin; NR: Norfolk Ridge; PNG: Papua New Guinea; PP:
1491 Papuan Peninsula; SFB: South Fiji Basin. Background image is ETOPO1 1 Arc-Minute Global
1492 Relief Model. (Amante and Eakins, 2009; NOAA National Geophysical Data Center, 2009).

1493 **B) Tectonic map.** Current tectonic plate names in blue. Current plate boundaries (Bird,
1494 2003) and plate boundary names in red, former plate names and plate boundaries in
1495 grey, suture of East Gondwana subduction zone in blue. Continental crust of Zealandia is
1496 outlined in yellow. Northland, New Caledonia, Louisiade, and Papuan Peninsula
1497 ophiolites are indicated by orange dots. Ontong Java Nui Large Igneous Provinces in
1498 light yellow. Lightblue lines are digitalized fracture zones, obtained from the GSFML
1499 database (Matthews et al., 2011; Seton et al., 2014; Wessel et al., 2015)

1500 AF: Alpine Fault; CP: Cocos Plate; EP: Easter Plate; GP: Galapagos Plate; HFZ: Hunter
1501 Fracture Zone; JF: Juan Fernandez Plate; MS: Manihiki Scarp; MTJ: Macquarie Triple
1502 Junction; NHT: New Hebrides Trench; NCT: New Caledonia Trench; SFZ: Shackleton
1503 Fracture Zone; SP: Scotia Plate; T-K-H: Tonga-Kermadec-Hikurangi; WARS: West Antarctic
1504 Rift System.



1505

1506

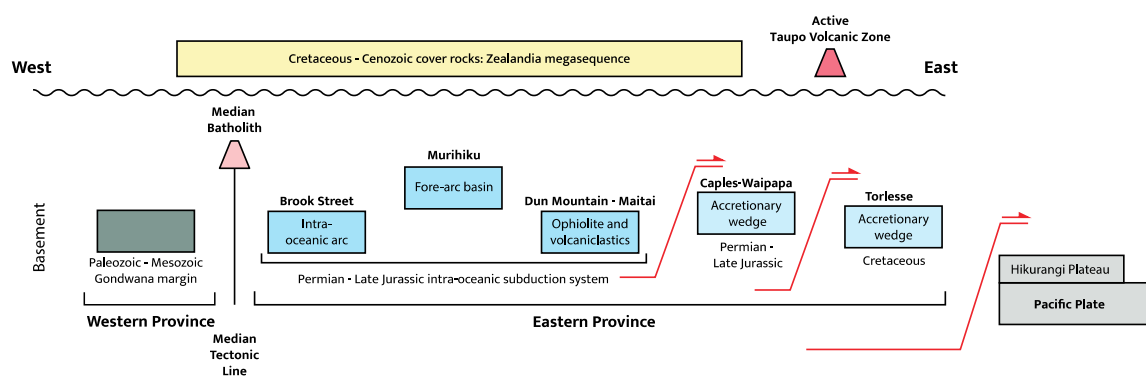
Fig. 2: Early Cretaceous (c. 140 Ma) reconstruction of the paleo-Pacific/Panthalassa realm showing the approximate extent of the Phoenix Plate. Continental crust of future Zealandia is outlined in black, highlighting the Zealandia margin of East Gondwana. Plate boundaries are only shown in the Panthalassa domain, dashed where the location of the plate boundary is estimated.

1507

1508

1509

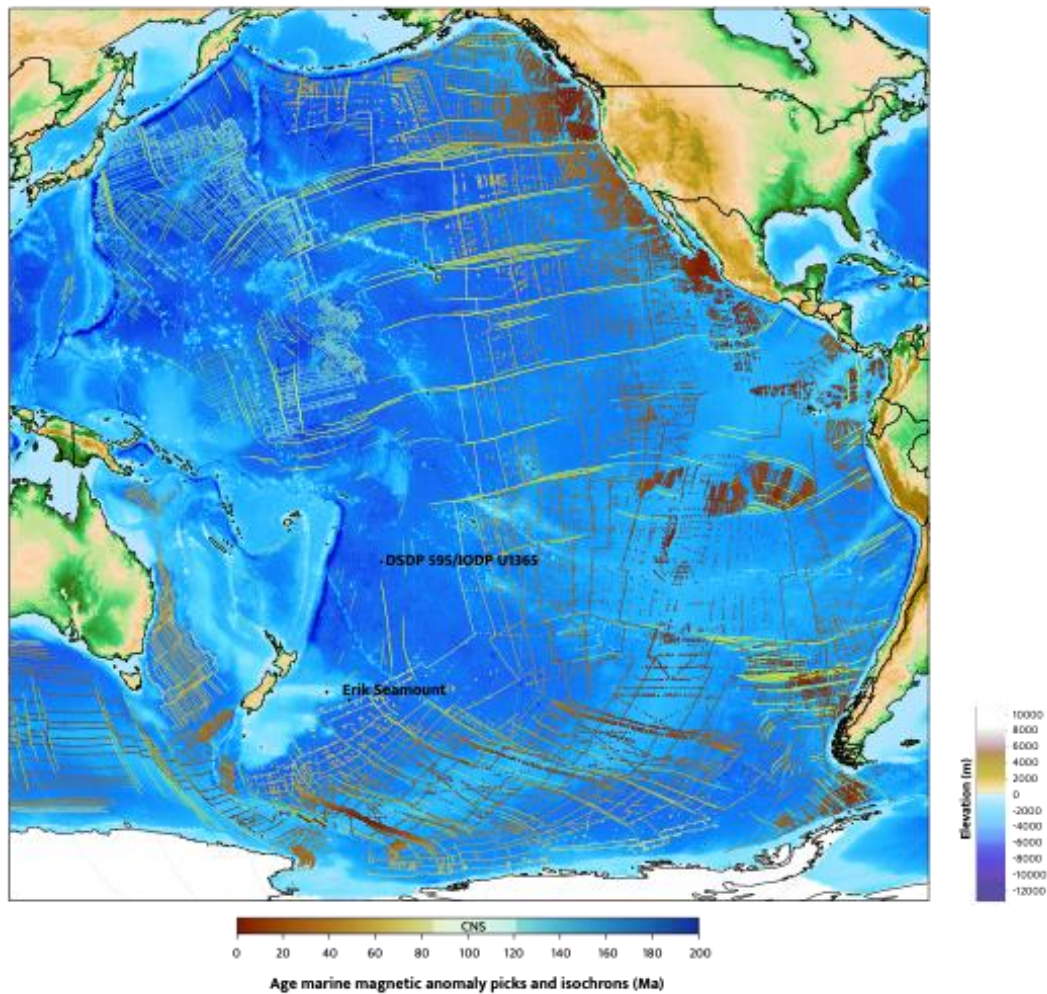
1510



1511

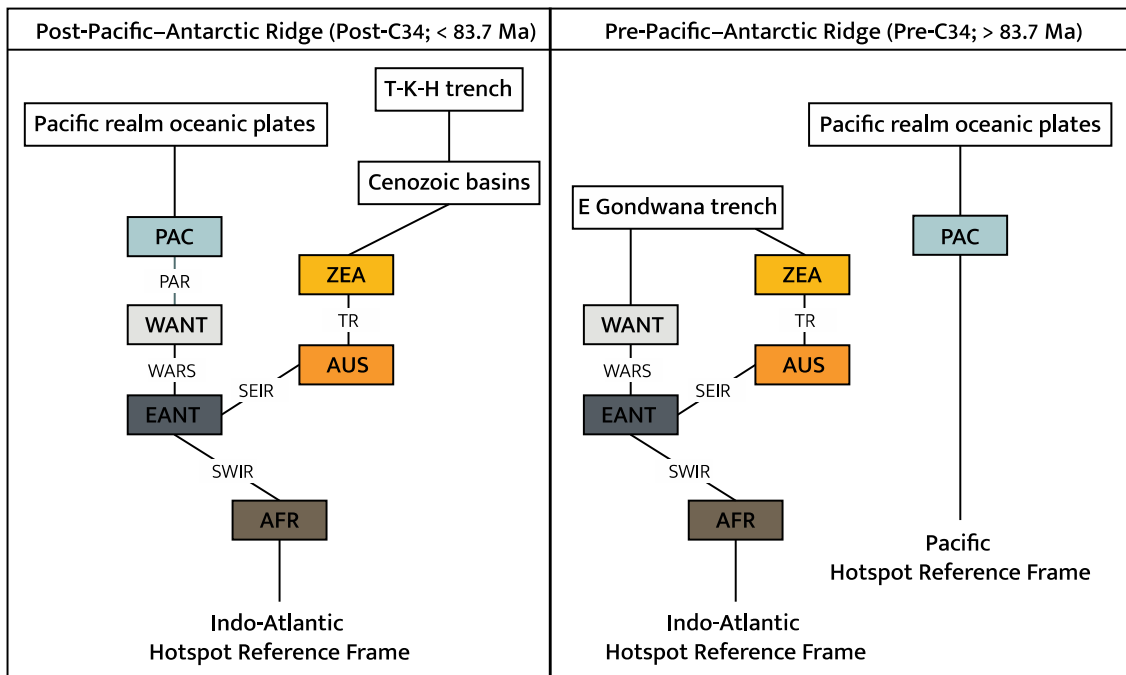
1512 **Fig. 3:** Schematic cross-section of the present-day geology of the North Island of New Zealand,
1513 based on Mortimer et al. (2014).

1514



1515

1516 **Fig. 4:** Geographic map of the Pacific and Southeast Indian oceans, showing the data used for the
1517 reconstruction of the oceanic domain. Marine magnetic anomaly picks (colored by age) and
1518 fracture zone data (in yellow) were obtained from the GSFML database (Seton et al., 2014, and
1519 references therein). Interpreted isochrons (in white) are from Seton et al. (2012), Wright et al.
1520 (2016), and from this study. Background image is ETOPO1 1 Arc-Minute Global Relief Model
1521 (Amante and Eakins, 2009; NOAA National Geophysical Data Center, 2009). Marine magnetic
1522 anomaly picks are colored using a color bar of Crameri (2018); Crameri et al. (2020)

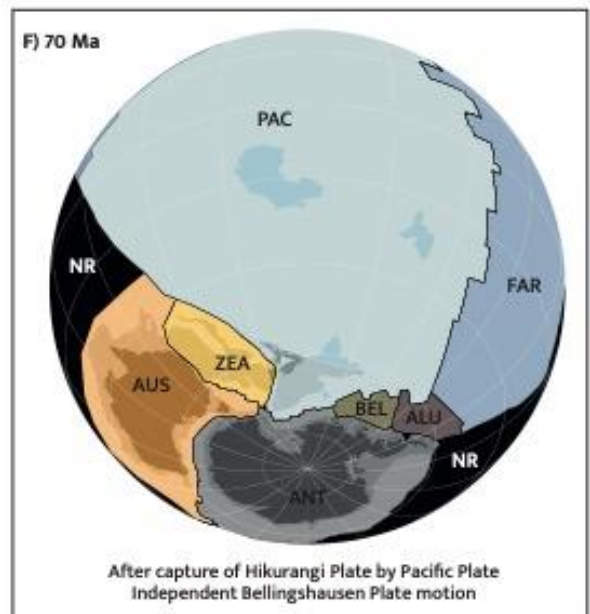
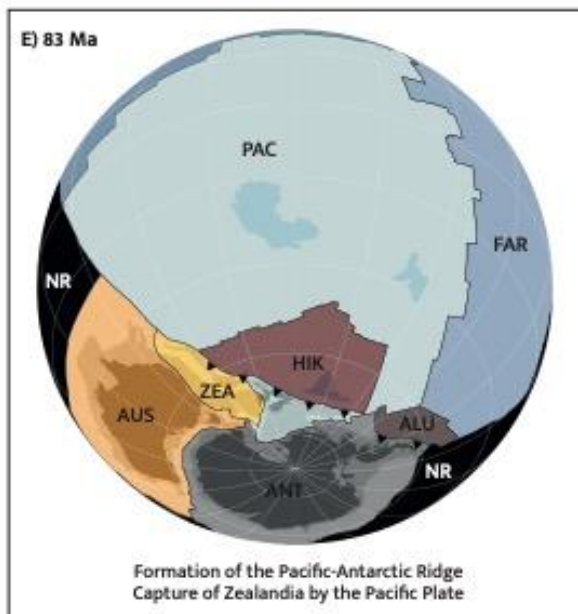
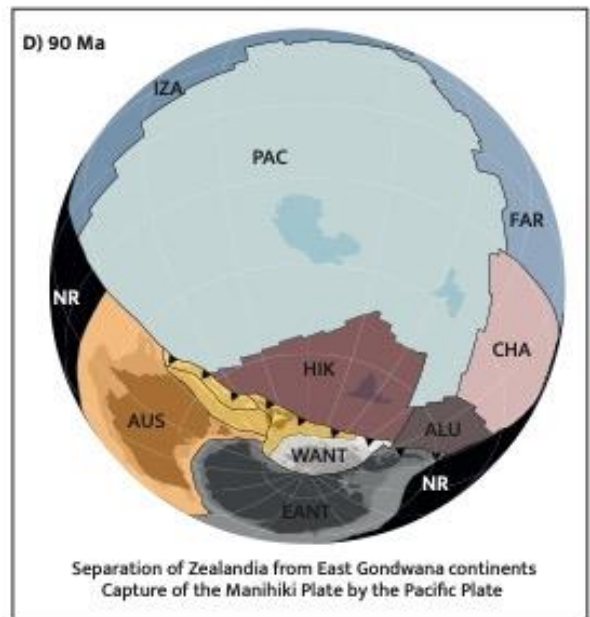
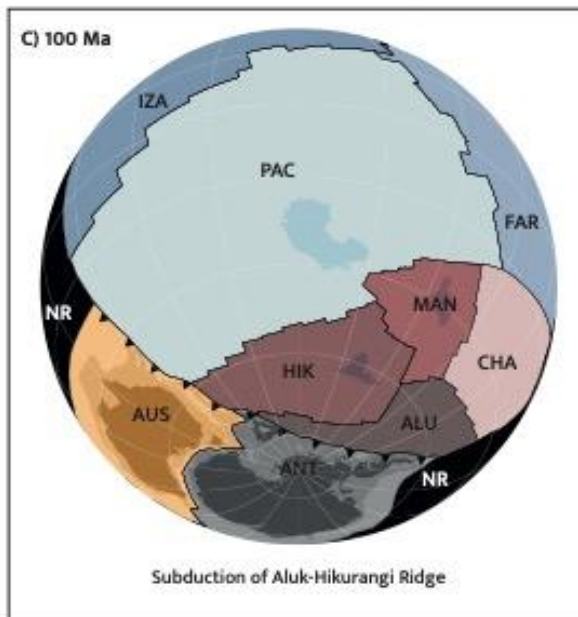
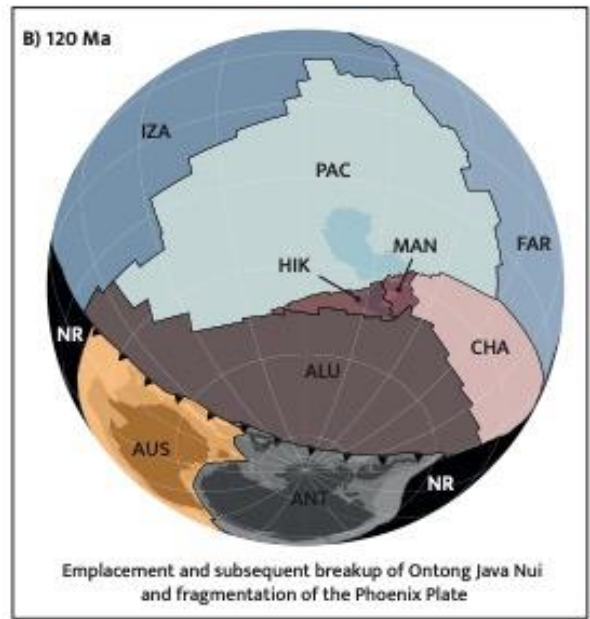
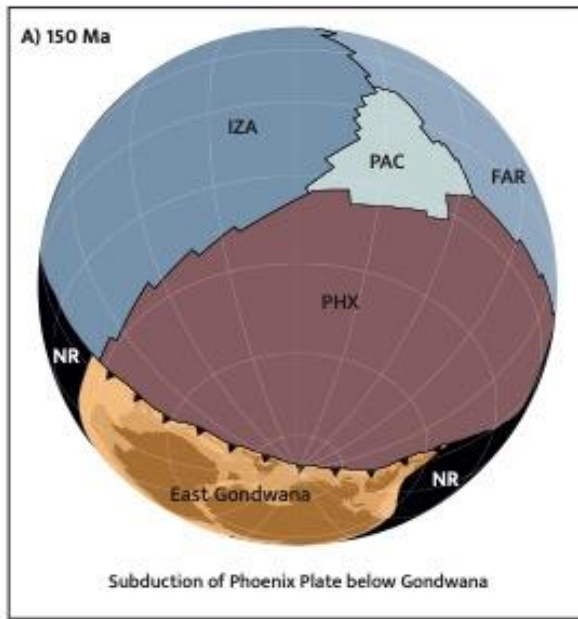


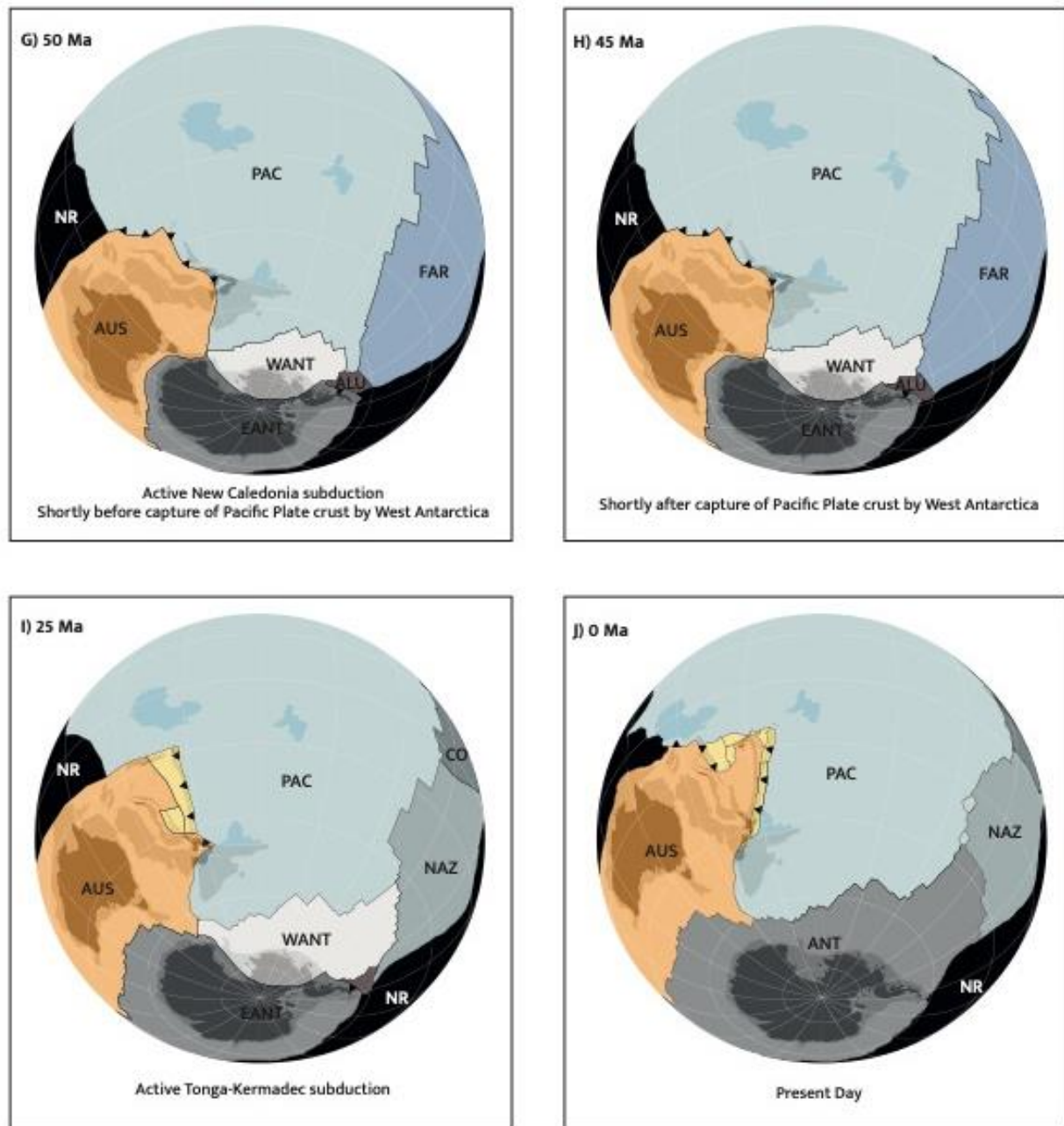
1523

1524 **Fig. 5:** Plate circuits used in our reconstruction, highlighting the differences in the plate circuit
 1525 before and after formation of the Pacific–Antarctic Ridge.

1526 *Plate names:* AFR: Africa; AUS: Australia; EANT: East Antarctica; WANT: West Antarctica; PAC:
 1527 Pacific; ZEA: Zealandia;

1528 *Plate boundaries:* PAR: Pacific–Antarctic Ridge; SEIR: Southeast Indian Ridge; SWIR: Southwest
 1529 Indian Ridge; TR: Tasman Ridge; T-K-H: Tonga–Kermadec–Hikurangi; WARS: West–Antarctic Rift
 1530 System.





1532

1533 **Fig. 6:** Snapshots of our kinematic reconstruction in the Van der Meer (2010) reference frame,

1534 highlighting key events in the evolution of the Phoenix Plate and East Gondwana subduction

1535 zone. These events are discussed in the main text. Present-day coastlines and outline of

1536 continental crust are shaded behind the plate colors and shown for reference. The Ontong Java

1537 Nui Large Igneous Provinces are also outlined, where the outline of the Hikurangi Plateau does

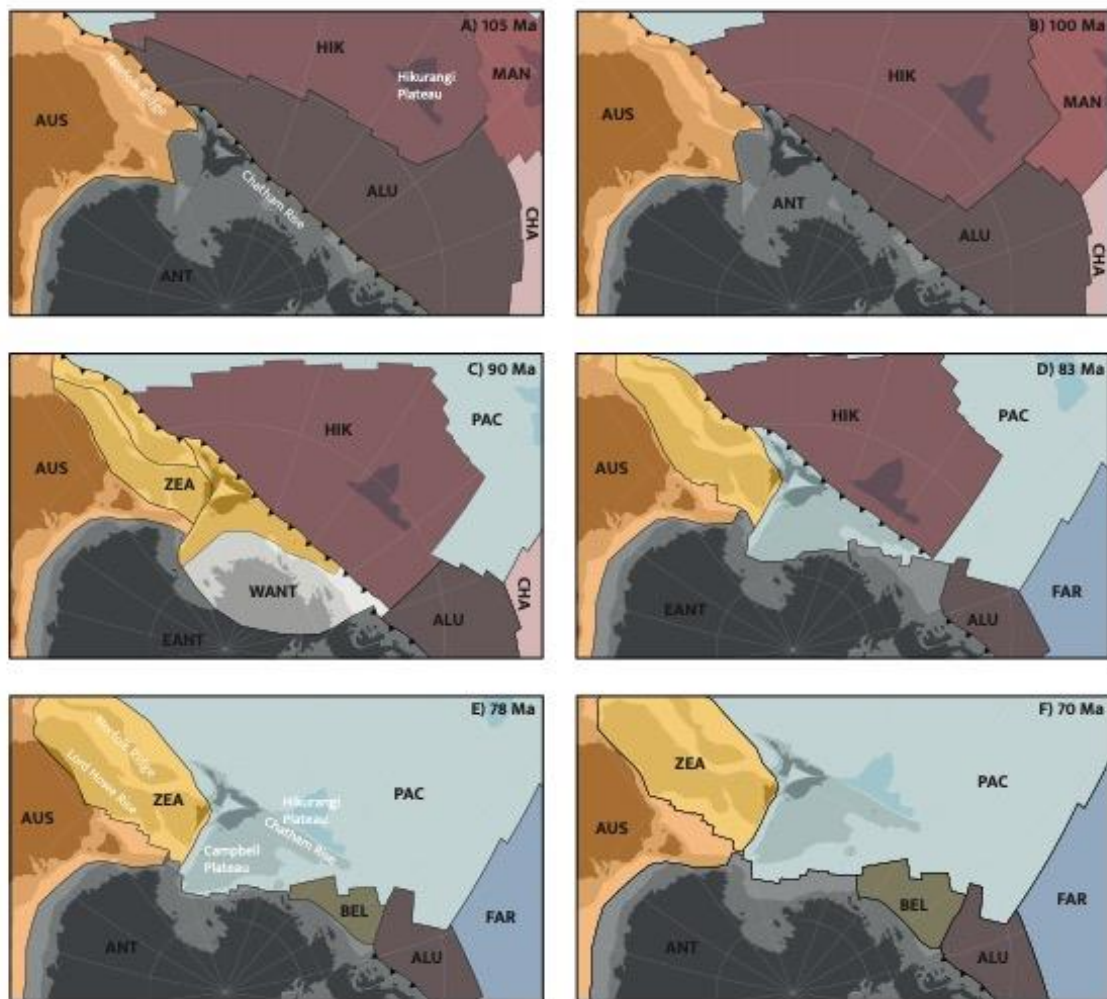
1538 not include the parts that were subducted below Chatham Rise and the North Island. Plate

1539 names: ALU: Aluk Plate; ANT: Antarctic Plate (EANT: East Antarctic Plate; WANT: West

1540 Antarctic Plate); AUS: Australian Plate; CHA: Chasca Plate; FAR: Farallon Plate; HIK: Hikurangi

1541 Plate; IZA: Izanagi Plate; MAN: Manihiki Plate; NAZ: Nazca Plate; PAC: Pacific Plate; SAM: South

1542 American Plate; ZEA: Zealandia. NR = Not Reconstructed.



1543

1544

1545

1546

1547

1548

1549

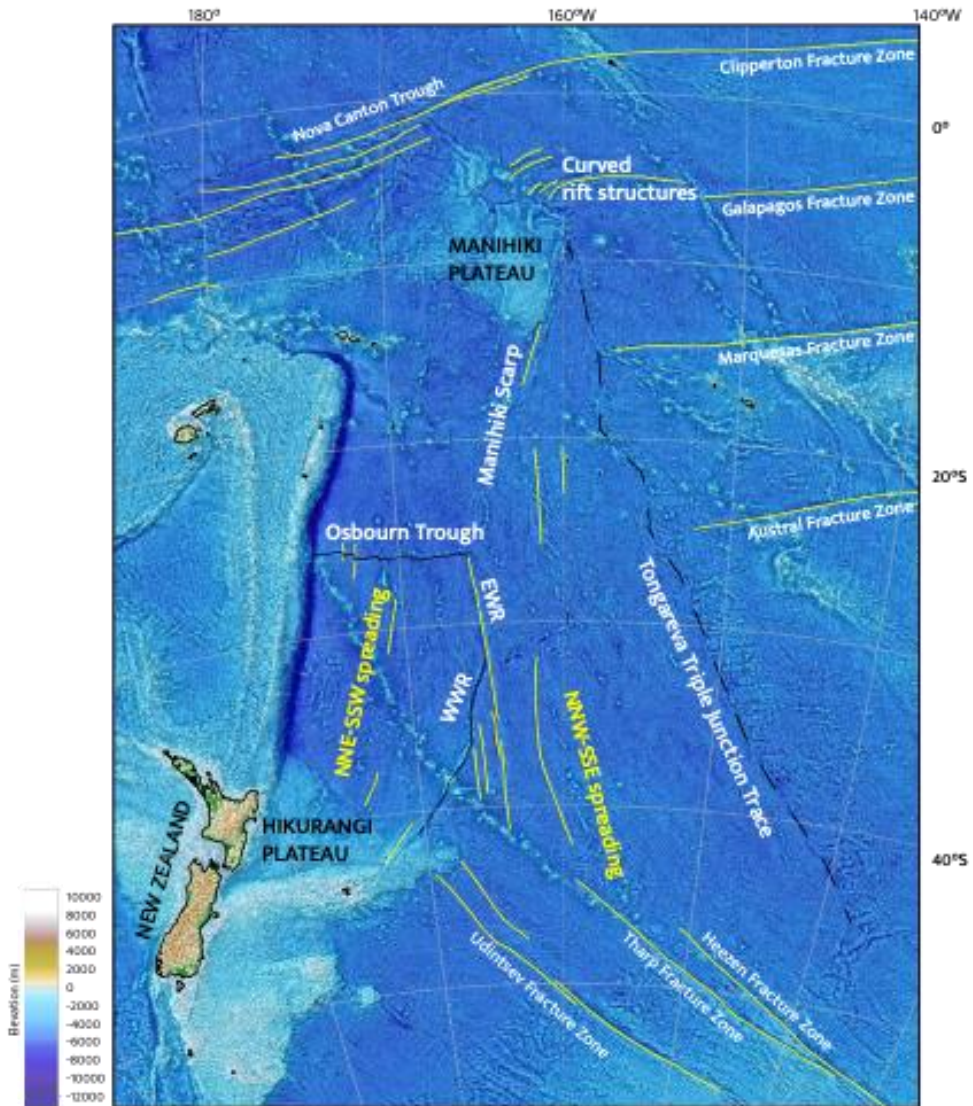
1550

1551

1552

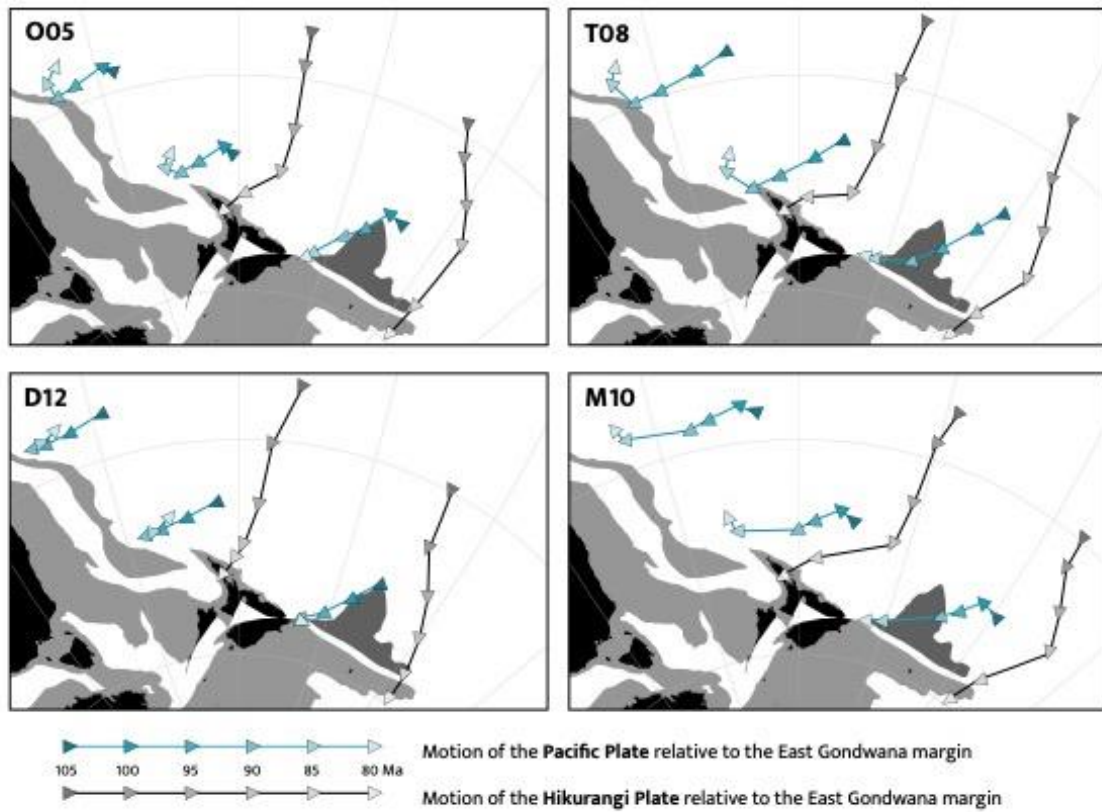
1553

Fig. 7: Detailed snapshots of our kinematic reconstruction in an East Antarctica fixed reference frame, highlighting the transition from the East Gondwana subduction zone margin to a passive margin. Extension within East Gondwana started in multiple locations before subduction of the Hikurangi Plate ended and this plate as well as Zealandia became part of the Pacific plate. Present-day coastlines and outline of continental crust are shaded behind the plate colors and shown for reference. The Ontong Java Nui Large Igneous Provinces are also outlined, where the outline of the Hikurangi Plateau does not include the parts that were subducted below Chatham Rise and the North Island. Plate names: ALU: Aluk Plate; ANT: Antarctic Plate (EANT: East Antarctic Plate; WANT: West Antarctic Plate); AUS: Australian Plate; HIK: Hikurangi Plate; MAN: Manihiki Plate; NAZ: Nazca Plate; PAC: Pacific Plate; ZEA: Zealandia.



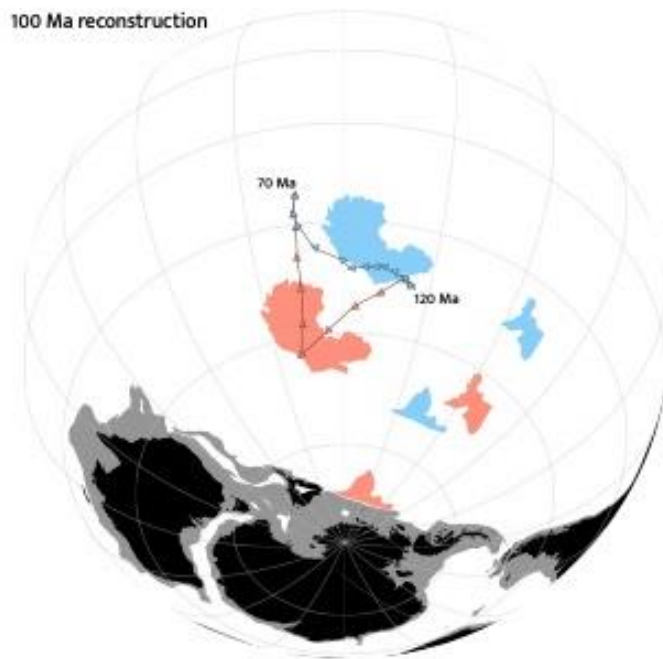
1554

1555 **Fig. 8:** Bathymetry of the region to the northeast of New Zealand, highlighting features of the
1556 seafloor fabric. Digitalized fracture zone data (in yellow) were obtained from the GSFML
1557 database (Matthews et al., 2011; Seton et al., 2014; Wessel et al., 2015). Background image is
1558 ETOPO1 1 Arc-Minute Global Relief Model (Amante and Eakins, 2009; NOAA National
1559 Geophysical Data Center, 2009).



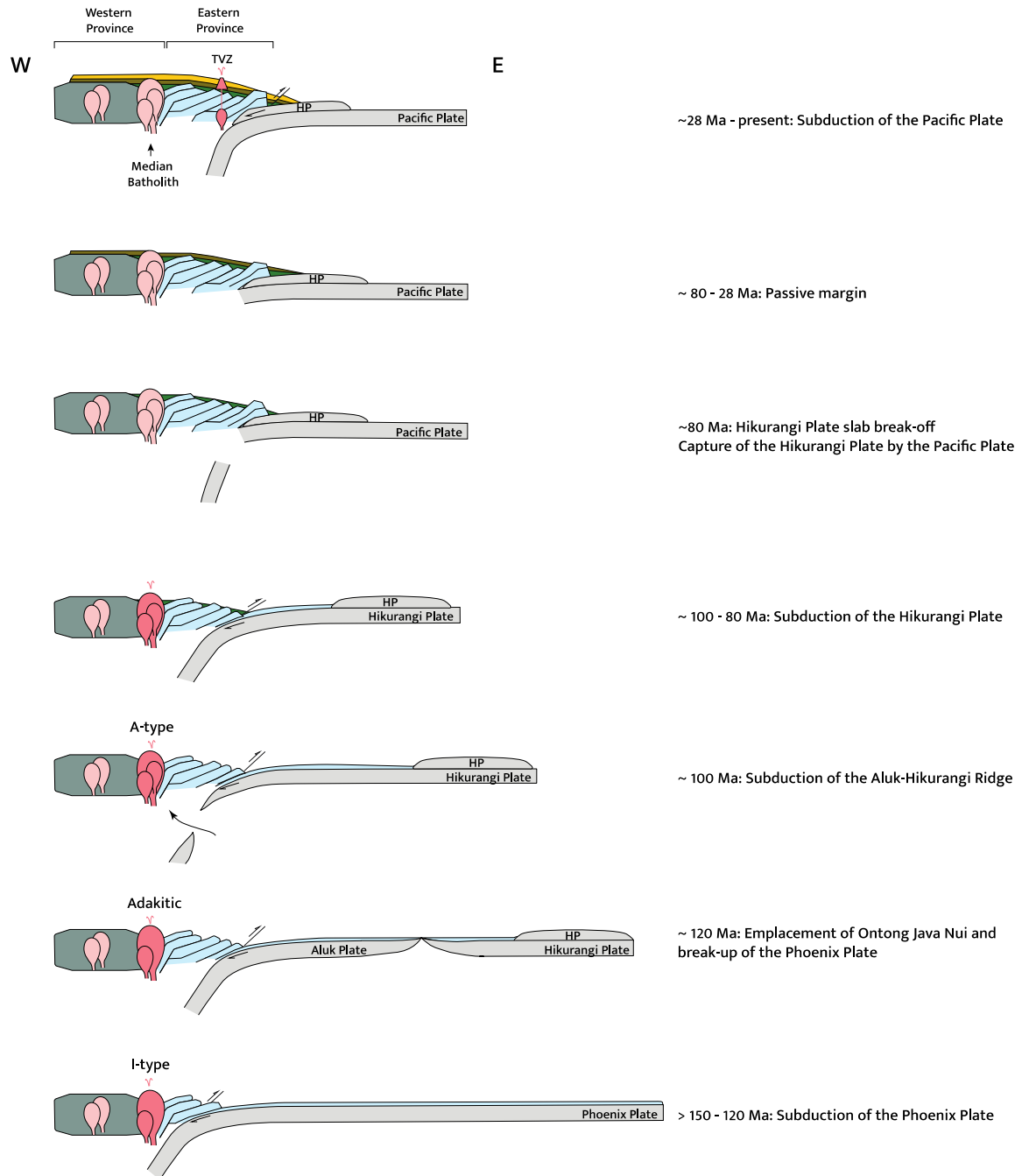
1560

1561 **Fig. 9:** 80 Ma reconstruction in an East Antarctica fixed reference frame showing the motion of
1562 the Pacific Plate and Hikurangi Plate relative to the East Gondwana margin in different mantle
1563 reference frames (O05: O'Neill et al., 2005; T08: Torsvik et al., 2008; D12: Doubrovine et al.,
1564 2012; M10: Van der Meer et al., 2010). This figure shows that convergence between the Pacific
1565 oceanic plates and the East Gondwana margin continued until at least 90 Ma in all reference
1566 frames, and until 79 Ma if Osbourn Trough spreading was still active.



1567

1568 **Fig. 10:** 100 Ma reconstruction that shows the difference in the location of the Pacific Plate
1569 between the hotspot reference frame of Torsvik et al. (2019) and the model of Mortimer et al.
1570 (2019) in which the Hikurangi Plateau arrives in the East Gondwana trench at 100 Ma. The
1571 difference is shown by the location of the LIPs, of which the Ontong Java Plateau has always
1572 been part of the Pacific Plate. In blue is the location of the LIPs as constrained by Torsvik et al.
1573 (2019), and in pink is the location of these plateaus in the model of Mortimer et al. (2019). Also
1574 shown are the 120-70 Ma motion paths of the Pacific Plate that result from the two models.



1575

1576 **Fig. 11:** Schematic cross-sections along the Zealandia margin to highlight the 150 Ma to present
 1577 tectonic history between the continental margin and the Pacific domain. The 28 Ma-present day
 1578 cross-section is across North Island, New Zealand, where the Hikurangi Plateau is presently
 1579 subducting, whereas older cross-sections are across the Chatham Rise where the Hikurangi
 1580 Plateau entered the trench in the Cretaceous. TVZ refers to the active volcanism of the Taupo
 1581 Volcanic Zone, which lies between the Waipapa and Torlesse terranes.